

Data Analysis in Electric Power System Embedded with Solar PVs

by

Mohammed Alzaid

A report

presented to University of Ontario Institute of Technology

In fulfillment of the

project requirement for the degree of

Master of Engineering

in

Electrical and Computer Engineering

Oshawa, Ontario, Canada, 2016

© Mohammed Alzaid, 2016

Abstract

Conventional source of energy are overly dependent on fossil fuel which tend to face several challenges such as the depleting of fossil fuel, environmental threat and human health. To deal with such challenges, solar PV system has been proposed to be embedded in the distribution system. Weather conditions plays a major role on affecting the power output of renewable energy sources, thus several power quality issues such as voltage variations are expected. Since the problem is of a stochastic nature, a probabilistic approach using Monte Carlo simulation techniques is adopted in this work. This project investigates the effect of PVs on residential house voltage and transformer power and Loss of Life through integrating rooftop solar PVs into the grid in such a way that the variations in the supply voltage caused by the solar irradiance and temperature remain within the acceptable limits set by IEEE Standards. In this respect, the analysis presented in this work also considers different scenarios including different penetrations of rooftop solar PVs (e.g., 0, 2, 4, 6, 8 and 10 kW), and the Monte Carlo algorithm is used to compute the impact of irradiance and temperature on the node voltages and transformer's power. The results of these scenarios reveal that with different PV penetrations, the node voltages of the houses supplied from 25 kVA transformers may experience more impacts compared to those houses supplied from 50 kVA transformers.

Acknowledgements

I would like to express deepest gratitude and thanks to my supervisor Dr. Walid Morsi Ibrahim for his full support, patience, guidance and encouragement throughout my study. Without his constant supervision and assistance, my project work would not have been feasible.

Besides my supervisor, I would also like to thank my fellow graduate students and friends who have willingly helped me out through this academic exploration.

Thanks also go to the Saudi Arabian Cultural Bureau in Canada for their financial support, help and supervision in order to finish this study.

Finally, an exceptional appreciation and thanks to my parents, wife, son and family for their patience, care, love and support during being abroad; I would not have been able to complete this project without their support, love and encouragement.

Table of Contents

Abstract	ii
Acknowledgments	iii
Table of Contents	iv
List of Figures	vii
List of Tables	x
List of Acronyms	xi
Chapter 1: Introduction	1
1.1 Motivation	1
1.2 Renewable Energy Sources	2
1.3 Power Quality Issues	2
1.4 Outline of the Chapters	4
1.5 Summary	5
Chapter 2: Renewable Energy	6
2.1 Introduction	6

2.2 Solar Photovoltaic	8
2.3 MicroFIT program	17
2.4 Voltage Quality	18
2.5 Summary	21
Chapter 3: Monte Carlo Methods	22
3.1 Introduction	22
3.2 Monte Carlo Fundamentals	22
3.3 Monte Carlo Simulation	24
3.4 Convergence issues	27
3.5 Summary	28
Chapter 4: Simulation & Results	29
4.1 Introduction	29
4.2 Primary Distribution System	30
4.3 Secondary Distribution System	31
4.4 System Description	32
4.5 System Data	34
4.6 Applying Monte Carlo Method	36
4.7 Secondary Results	37
4.8 Summary	57

Chapter 5: Conclusions	58
5.1 Conclusions	58
References	60
Appendix A IEEE 34-Bus Standard Test Distribution System Data	65
Appendix B Secondary System Data	69
Appendix C Transformer Insulation Life	70

List of Figures

Figure 2.1: Renewable energy for EU countries in 2010 and commitment for 2020	7
Figure 2.2: Schematic of a PVT collector	8
Figure 2.3: Direct and diffuse radiation	9
Figure 2.4: Solar cell, module and array	10
Figure 2.5: Principles of photovoltaic cell	11
Figure 2.6: I-V and P-V characteristics of PV cell	12
Figure 2.7: Basic principles of a PV solar energy system	15
Figure 2.8: Schematic diagram of a direct-coupled PV system	15
Figure 2.9: Schematic diagram of a stand-alone PV application	16
Figure 2.10: Schematic diagram of a grid-connected system	16
Figure 2.11: Schematic of microFIT program	17
Figure 2.12: General structure of grid-connected PV system	18
Figure 2.13: Variation of PV system power output during: (a) sunny day and (b) cloudy day	19
Figure 2.14: Center-tapped distribution transformer.....	20
Figure 3.1: Equivalent circuit pf the PV module	25
Figure 3.2: Value converges by using Monte Carlo technique	28
Figure 4.1: Power generation, transmission and distribution	30

Figure 4.2: Generalized Distribution System	30
Figure 4.3: A 25 kVA distribution transformer with 6 houses	31
Figure 4.4: A 50 kVA distribution transformer with 10 houses	31
Figure 4.5: Modified IEEE 34-Bus standard test system	32
Figure 4.6: Monthly Temperature in Toronto, Canada	34
Figure 4.7: Variation of PV system power output during applying different scenarios & 50KVA	37
Figure 4.8: Variation of PV system power output during applying different scenarios & 25KVA	38
Figure 4.9: Convergence based on mean value of home voltage	39
Figure 4.10: Convergence based on mean value of transformer power	40
Figure 4.11: Convergence based on mean value of home voltage	42
Figure 4.12: Convergence based on mean value of transformer power	43
Figure 4.13: Convergence based on mean value of home voltage	45
Figure 4.14: Convergence based on mean value of transformer power	46
Figure 4.15: Convergence based on mean value of home voltage	48
Figure 4.16: Convergence based on mean value of transformer power	49
Figure 4.17: Convergence based on mean value of home voltage	51

Figure 4.18: Convergence based on mean value of transformer power	52
Figure 4.19: Convergence based on mean value of home voltage	54
Figure 4.20: Convergence based on mean value of transformer power	55

List of Tables

Table 1.1: Categories of power quality problems	3
Table 2.1: PV efficiencies	10
Table 4.1: Toronto Temperature Data	34
Table 4.2: Center Tapped Distribution Transformer Parameters	35
Table 4.3: Modified IEEE 34-Bus Standard Test System	36
Table 4.4: Transformer Loading	38
Table 4.5: Transformer Loss of Life during the year	41
Table 4.6: Transformer Loss of Life during the year	44
Table 4.7: Transformer Loss of Life during the year	47
Table 4.8: Transformer Loss of Life during the year	50
Table 4.9: Transformer Loss of Life during the year	53
Table 4.10: Transformer Loss of Life during the year	56

List of Acronyms

AC	Alternating Current
CWEED	Canadian Weather Energy Engineering Datasets
CSP	Concentrated Solar Power
DC	Direct Current
DER	Distributed Energy Resources
DG	Distributed Generation
EU	European Union
FIT	Feed-in Tariff
IESO	Independent Electricity System Operator
IEEE	Institute of Electrical and Electronic Engineers
KV	Kilovolts
LOL	Loss of Life
MCMC	Markov Chain Monte Carlo
MC	Monte Carlo
PV	Photovoltaic
PCC	Point of Common Coupling
PVT	Hybrid Photovoltaic-Thermal
PES	Power and Energy Society
PCC	Point of Common Coupling
PQ	Power Quality
RERs	Renewable Energy Resources

RESs	Renewable Energy Sources
SDs	Service Drops
SLs	Service Lines
SAPS	Stand-Alone Power Systems

CHAPTER 1

INTRODUCTION

1.1 Motivation

The growth in worldwide demand for energy sources such as oil and gas has reduced due to the concern about the environmental issues associated with conventional sources. However, shifting toward renewable energy such as solar, wind, nuclear has increased greatly especially with the implementation of smart grid. A smart grid is an evolved grid system that uses digital technology to improve the system efficiency, reliability, security and economically. Recently, the quantity of distributed generators (DGs) which is the electric generation facilities connected to distributed network are also promptly increasing. The privileges of DGs resources penetration in distributed network can be summarized as loss reduction, delayed investment for developing network and improvement in reliability [1-2].

Unlike traditional sources, renewable-based DGs are not “dispatchable”, and the power output is challenged to control because of the variability resulting from weather conditions. However, smart grids promise to provide benefits and facilitate the integration of renewable energy [1].

Solar energy is quickly becoming an alternative means of electricity source. The depleting of fossil fuels are serious issue, thus the need for alternative energy source is a necessity, especially for consumers who live in destitute areas and struggle to have access to electricity distribution

networks. In fact, one of the difficulties that photovoltaic systems (PV) face is the “changing of output power due to variations in temperature and irradiance, which directly affects the load that is connected to photovoltaic systems” [3]. This project is intended to investigate the issue of variability on PV power output during the year and its effect on the load that is connected.

1.2 Renewable energy sources

Conventional energy sources are considered as the drivers in terms of the economic progress. However, they are damaging the environment and human health because they are based on fossil fuel such as oil, natural gas and coal. Unlike traditional sources, renewable energy sources (RESs) such as solar, wind, biomass, hydropower and geothermal are very clean sources and can meet the world’s energy demand. They provide sustainable energy services and consume resources that are routinely available in nature [4]. As stated in [5], the renewable energy resources (RERs) in some countries represent around 20% of the total generation capacity. Furthermore, by 2030, they will provide as twice as the nuclear share out of total sources [5].

1.3 Power quality issues

Electric power quality (PQ) is defined “as the goodness of the electric power quality supply in terms of its voltage wave shape, its current wave shape, its frequency, its voltage regulation, as well as level of impulses, and noise, and the absence of momentary outages” [6]. Renewable energy sources depends on the scale of power generation when they are integrated. Small scale power generations are always connected to distribution systems. However, large scale distributed

power generation is connected to transmission systems. Both types face certain challenges during the integration [7]. According to [8], the challenges such as voltage regulation, harmonic distortion, stability, and flicker are the power quality issues that can occur at the generation, transmission and distribution. Table 1.1 shows the other classifications of power quality problems that are associated to the source of supply and types of load. As reported by [9], faulty connection and wiring represent 70-80% of all power quality related problems.

Power Freq Disturbance	Electro Magnetic Interferences	Power System Transient	Power System Harmonics	Electrostatic Discharge	Power Factor
<ul style="list-style-type: none"> • Low Freq phenomena • Produce Voltage sag / swell 	<ul style="list-style-type: none"> • High freq phenomena • interaction between electric and magnetic field 	<ul style="list-style-type: none"> • Fast, short-duration event • Produce distortion like notch, impulse 	<ul style="list-style-type: none"> • Low frequency phenomena • Produce waveform distortion 	<ul style="list-style-type: none"> • Current flow with different potentials • Caused by direct current or induced electrostatic field 	<ul style="list-style-type: none"> • Low power factor causes equipment damage

Table 1.1: Categories of power quality problems [9]

The economic impact of power quality problems are grouped into three classes; direct impact such as loss of production, equipment damage, environmental penalties and human health and safety; indirect impact such as financial cost of loss market; and social impact such as personal injury [10]. Mitigate the power quality problem has two ways, either from the utility side or customer side. Installing line conditioning systems is the first solution to counteract the power system disturbances. The other approach is the load conditioning that confirms the equipment is not high sensitive to power disturbances [9].

1.4 Outline of the chapters

This report is organized as follows:

Chapter 1 presents the motivation behind the project. Moreover, a general concept of renewable energy is briefly presented followed by different power quality issues that may affect the integration of renewable energy to the grid.

Chapter 2 presents the main concept of renewable energy along with solar architecture. The characteristics and operation systems of solar are discussed in details including their way to grid connection. MicroFIT Program in Canada is expressed with its rules of eligibility. Moreover, various voltage quality issues that affect the integration of PV are also presented.

Chapter 3 presents an in-depth introduction to Monte Carlo methods including the fundamentals and simulation. Various issues associated with the convergence of Monte Carlo are also explained in detail.

Chapter 4 provides six scenarios modeled and simulated in MATLAB and Open-DSS. The results provided in details the impact of varying PVs on house voltage and transformer power. Moreover, the yearly Loss of Life of both transformer 50 kVA and 25 kVA are calculated.

Finally, Chapter 5 concludes the work presented in this project report including the results.

1.5 Summary

This chapter presents an overview of renewable energy sources along with different power quality issues that may degrade the integration of renewable energy to the grid. Possible mitigation solutions that will be investigated later are highlighted. Chapters outline is also included which shows the structure of the report.

Literature Review

RENEWABLE ENERGY

2.1 Introduction

Renewable energy is the energy that comes from resources which are replenish themselves and not depleted by continued use. Solar, hydropower, wind, geothermal, biofuels, and biomass are some examples of the renewable energy sources. Concerns about the environmental consequences resulting from the use of fossil fuel, such as the increasing emissions of air pollutants and global climate change has pushed the renewable energy to grow dramatically, since they are less environmentally destructive than the conventional energy sources [11-12].

According to [13], the advantages of renewable energy sources are as follows:

- a) Reducing dependency on fossil fuels.
- b) Addressing environmental issues.
- c) Reliability of electric power system.
- d) Decreasing operation costs.
- e) Power quality.
- f) Energy security.
- g) Conservation of natural resources.

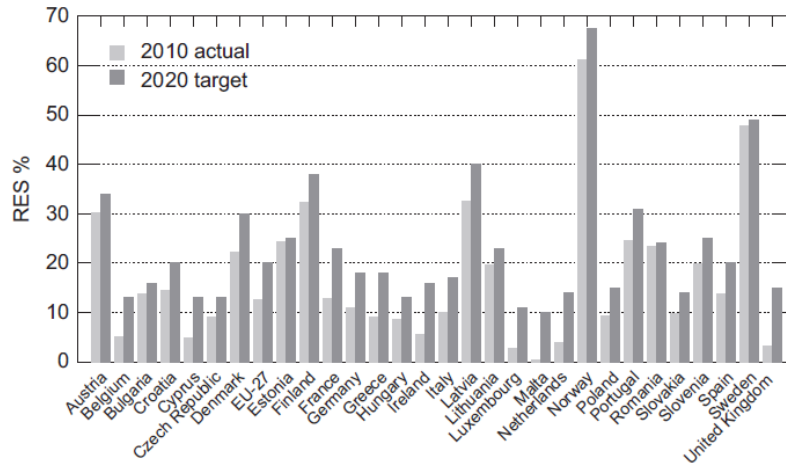


Figure 2.1: Renewable energy for EU countries in 2010 and commitment for 2020 [13]

Sustainable energy for European Union (EU) member countries in 2010 compared to the prediction in 2020 is shown in Figure 2.1. According to [12], the major target of the EU countries is to reduce the carbon emission 20% and increasing the final energy consumption of renewable energy 20% by 2020. Therefore, that will be a major factor in the growing use of the sustainable energy technology by the latter half of the twenty-first century.

Renewable energy sources are known as a “Distributed Generation” (DG) when they are incorporated into the distribution network. Literature [14] defines the DG as the generation of electricity that provides at sites closer to customers. The electricity source can be solar photovoltaic cells, wind, gas turbines, fuel cells, or biomass and known as “Distributed Energy Resources” (DER) [11]. The DG can benefit to a facility, such as electric cost reduction, increasing reliability of power supply, less transmission loss, easy start and stop, and improving disaster level [11-15]. The result in [15] proved the effective and feasible approach of DG system based on various renewable energy resources due to its specific distribution characteristics, no big effect to the grid, and direct power supply to the local loads.

2.2 Solar Photovoltaic

Solar photovoltaic (PV) is defined as a technology that converts solar energy directly into electricity. As stated in [16], there are two main forms for solar radiation to be utilized. First, solar cells which converts the sun's arrays directly to electricity, often known as photovoltaic. This form of utilizing energy is generally specified by their peak electrical output [12]. Second, concentrated solar power (CSP) which is basically collecting heat by capturing the sunlight to produce electricity indirectly. Unlike the solar cells, solar collectors are specified by their peak thermal output [12]. According to [17], these two forms can be combined together to produce both electricity and heat at the same time, so this combination is known as hybrid photovoltaic-thermal (PVT) collector system. Figure 2.2 below shows the schematic of a PVT collector.

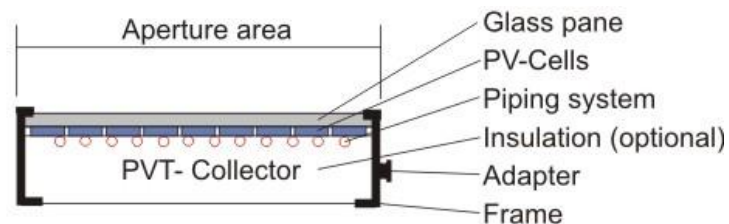


Figure 2.2: Schematic of a PVT collector [17]

PV solar energy has advantages and drawbacks as similar as every energy source seen today. However, its advantages overcome the disadvantages as includes in the following: environmentally friendly, works without fuels, lifetime up to 30 years, no emissions, no noise, operates in any weather conditions, required minimal maintenance, and whenever there is solar, light, electricity is generated [16].

2.2.1 Photovoltaic Cells

At present, PV devices are commonly based on silicon. The direct current (DC) flows when the devices are exposed to the sun. PVs respond to either direct or diffuse radiation as shown in figure 2.3. In addition, their output increases with increasing irradiance and decreases with rising temperature [18].

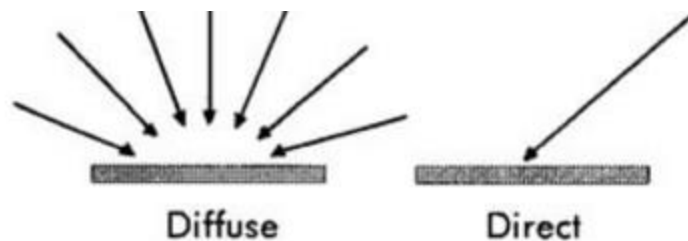


Figure 2.3: Direct and diffuse radiation [18]

In a PV system, cells are connected to each other to form modules. Therefore, this combination gives the flexibility to the system to be either expanded or reduced to suit any given application. Modules are intended to supply electricity at a certain voltage, such as 12 volts system as common, and to form an array, multiple modules can be wired together as shown in figure 2.4. Generally, whenever the area of a module or array is increased, electricity will be produced more. Nowadays, monocrystalline silicon, polycrystalline silicon and thin film silicon are the most common PVs available. Table 2.1 represents efficiencies of the three common PVs [18-20].

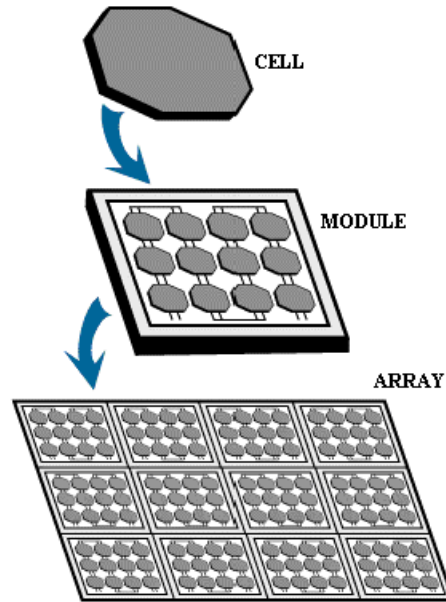


Figure 2.4: Solar cell, module and array [20]

Type	Approximate cell efficiency %	Approximate module efficiency %
1. Monocrystalline silicon	13 – 17 (1)	12 – 15 (2)
2. Polycrystalline silicon	12 – 15 (1)	11 – 14 (2)
3. Thin-film silicon (using amorphous silicon)	5 (3)	4.5 – 4.9 (2)

Table 2.1: Solar photovoltaic (PV) efficiencies [18]

2.2.1.1 Principles of Photovoltaic Cell

The operation of a basic PV cell is demonstrated in Figure 2.5. Solar cells are usually made of silicon as same as the semiconductor materials. The thin semiconductor wafer has a positive (backside) and negative (front side) in different sides in order to form an electric field. Electrons are knocked loose from the atoms in the semiconductor material when the light energy strikes the solar cell. Therefore, the electrons can be captured in the form of an electric current when the

electrical conductors are attached to the positive side and negative side, which forming an electrical circuit. In this case, the electric current is actually electricity that can be used to power a load, such as a light [20].

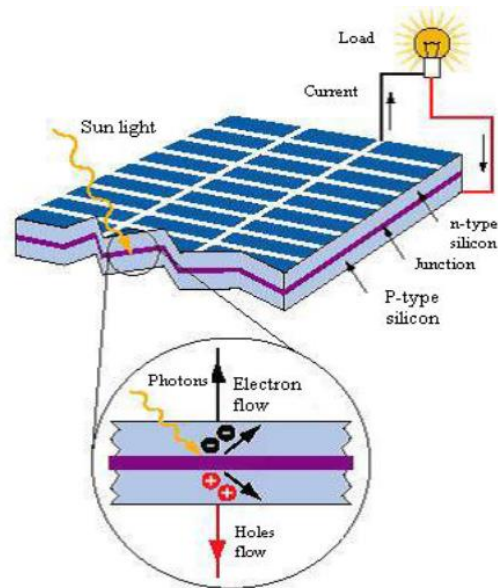


Figure 2.5: Principles of photovoltaic cell [19]

2.2.1.2 Solar Photovoltaic (PV) Cell Characteristics

A typical I-V characteristics of the solar cell is shown in figure 2.6. The straight line with the slope ($I/V=1/R$) in the curve is the load characteristics. It is seen that the power supplied to the load depends only on the value of the resistance. However, the cell operates in the region M-N when the load R is small. This shows that the cell behaves as a constant current source (almost equal to the short circuit current). On the other hands, the cell operates in the region P-S when the load R is large. In this case, the cell behaves as a constant voltage source (almost equal to the open circuit voltage) [21].

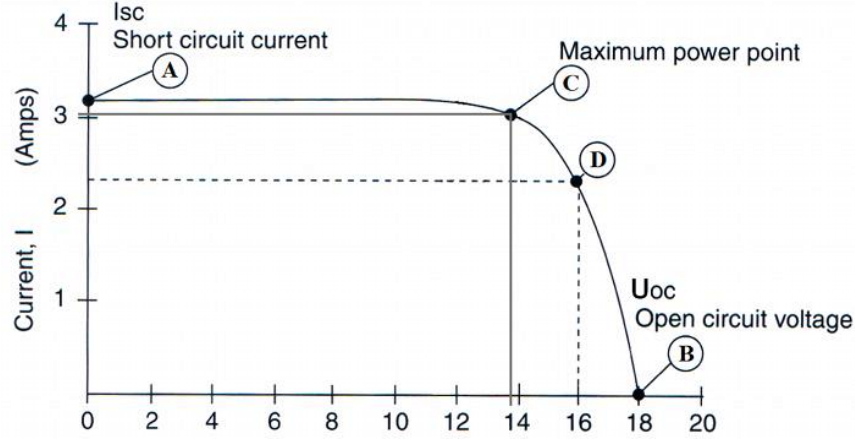


Figure 2.6: I-V characteristics of PV cell [21]

Fundamental parameters of a real solar cell is characterized by the followings [21]:

- **Short circuit current:** the cell generated the best value of the current ($I_{sh}=I_{ph}$). This will be produced by the short circuit conditions ($V=0$).
- **Open circuit voltage:** when the generated current is $I=0$, it matches the voltage drop across the (p-n junction) diode. Therefore, it reflects the cell voltage at night and can be expressed mathematically as:

$$V_{OC} = \frac{nkT}{q} \ln \left(\frac{I_L}{I_0} \right) = V_t \ln \left(\frac{I_L}{I_0} \right) \quad (2.1)$$

Where T is the absolute cell temperature and $V_t = \frac{mkT_c}{e}$ is the thermal voltage.

- **Maximum power point:** the operating point A (V_{max} , I_{max}) when the power dissipated in the resistive load is maximum ($P_{max}= V_{max} * I_{max}$).
- **Maximum efficiency:** the ratio between the maximum power (P_{max}) and the incident light power (P_{in}):

$$\eta = \frac{P_{max}}{P_{in}} = \frac{I_{max} V_{max}}{A G_a} \quad (2.2)$$

Where A is the cell area and G_a is the ambient irradiation.

- **Fill factor:** the ratio of the maximum power. For good cells, the value often is higher than 0.7. As the solar cell temperature increases, the fill factor is diminished [22].

$$FF = \frac{P_{max}}{V_{OC} I_{SC}} = \frac{I_{max} V_{max}}{V_{OC} I_{SC}} \quad (2.3)$$

2.2.2 Factors that Affect Solar Cell Efficiency

Solar Cells output are affected by weather and seasonal variation. The efficiency of solar panel is around 14 -18%. Some factors such as no enough sunlight, changing the strength of the sun and temperature contribute to less efficiency to the solar cell.

2.2.2.1 Effect of Sunlight on Solar Cell's Performance

Sunlight is considered as a major effect on the solar cell performance. The output of the solar cell is decreased relatively when the power density of the sunlight is decreased. The reason for that such decreases is due to the sun is not shining directly on the cell or there is no enough sunlight because of sunrise or sunset. According to [6], solar cell should be tilted south by the angle of the latitude of the location on the earth in order to get a maximum energy absorption from the sun.

2.2.2.2 Effect of Changing Strength of the Sun on a Solar Cell

The effects of the variation in power density is usually included in the characteristics of a solar cell. It is known that the output DC current is directly proportional to the intensity of the sunlight. However, the voltage output is relatively independent on the sunlight under open circuit

conditions. We can conclude that when the power density varies, the effect of the load on the operating point is more important [6].

2.2.2.3 Effect of Temperature on Solar Cell Characteristics

The output of a solar cell is function to its cell temperature. The current increases when the temperature increases, while the voltage decreases by about $2.1 \text{ mV}/^\circ\text{C}$. Consequently, the power output and the cell efficiency will decrease. The voltage and current of the cell are determined from the following relations respectively [6]:

$$E_0 = E_R - 0.0021 (T - 25) \quad (2.4)$$

$$I_0 = I_R - 0.025A (T - 25) \quad (2.5)$$

Where E_R and I_R are the cell ratings in volts and milli-amperes at 25°C . T is the new temperature, and A is the cell area in square centimeter [6].

2.2.3 Applications

PV modules are well designed to be suitable for outdoor use under severe conditions, such as marine and desert environments. Power modules are commonly having around 50-180 W each as a rated power output. Figure 2.6 shows the basic principles of a PV solar energy system. It is easy to see that the PV array produces electricity that can be controlled by the controller to either battery

storage or a load. When there is no sunlight, the battery has the ability to supply power to the load as long as it has a satisfactory capacity [22].

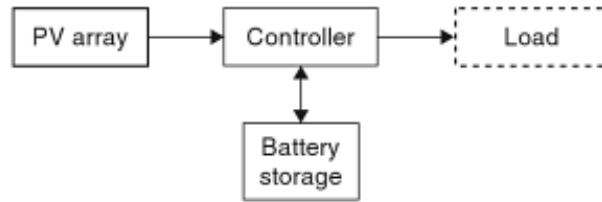


Figure 2.7: Basic principles of a PV solar energy system [22]

2.2.3.1 Direct-coupled PV System

PV arrays is directly connected to the load in the direct-coupled PV System. Therefore, the load can be operated only when there is a sunlight. Water pumping is the typical application for this type of system. Figure 2.7 shows the schematic diagram of a direct-coupled PV system [22].



Figure 2.8: Schematic diagram of a direct-coupled PV system [22]

2.2.3.2 Stand-alone Applications

According to [22], a stand-alone power systems (SAPS) are used in remote areas where there is no access to an electricity grid. In this system, the produced energy is normally stored in batteries. In addition, AC and DC loads can be satisfied simultaneously. Figure 2.8 shows the schematic diagram of a stand-alone PV system.

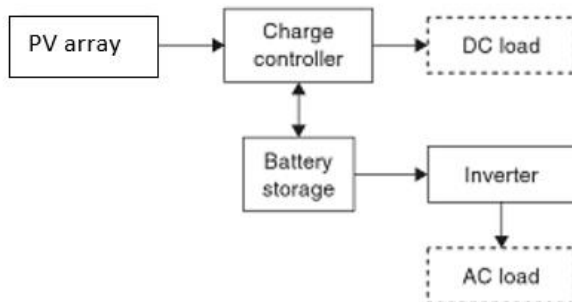


Figure 2.9: Schematic diagram of a stand-alone PV application [22]

2.2.3.3 Grid-connected System

Recently, PV system is usually connected to the local electricity network. During the day, the generated electricity can either be used immediately or sold to the electricity company. During night, power can be bought back from the grid when the solar system cannot provide the electricity required. In this case, the solar system does not contain battery storage because the grid is acting as an energy storage system. Figure 2.9 shows the schematic diagram of a grid-connected system [22].

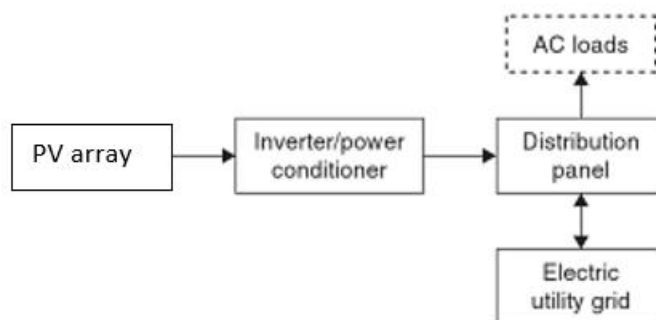


Figure 2.10: Schematic diagram of a grid-connected system [22]

2.3 MicroFIT Program

In 2009, the Ontario government in Canada established the microFIT program that managed by the IESO (Independent Electricity System Operator) in order to increase renewable energy in the province [23-24]. According to [24], that will allow homeowners to generate their own electricity and based on the amount of solar energy production, they will receive a government income. Homeowners are allowed to install up to 10 Kilowatt of energy on the rooftop as shown in figure 2.13. Therefore, participants are being paid a fixed price around 40 cents per kilowatt over a 20 year term for the electricity they will produce and deliver to the province's electricity grid [23-24].

People must follow the following rules to be eligible for the microFIT program [23]:

- Use renewable fuel such as biogas, biomass, solar PV, wind, waterpower, and landfill gas
- Must be Ontario residents
- Be connected to the IESO controlled grid
- Have separate meter

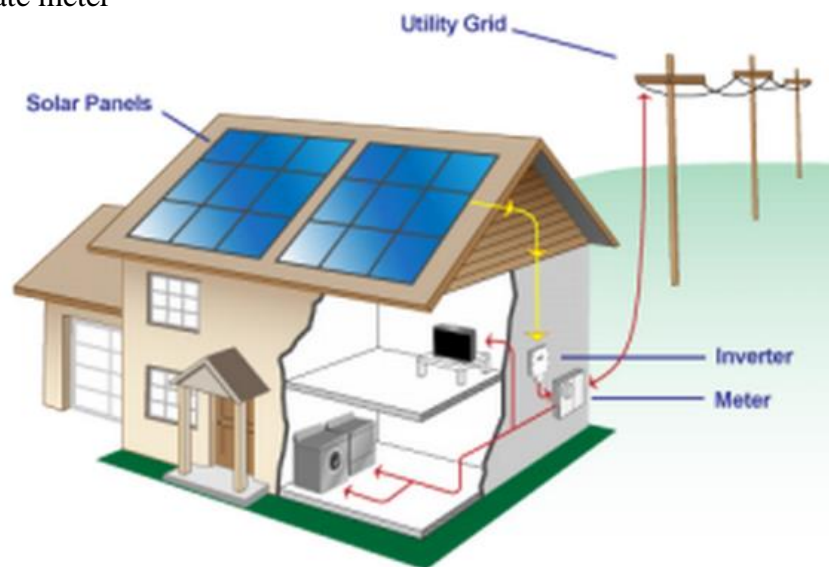


Figure 2.11: Schematic of microFIT program [24]

2.4 Voltage Quality

The efficiency and proper operation of renewable energy are very important and depend on some factors. Solar system will be used in this section as an example of voltage quality on renewable energy. In PV system, environmental conditions and system design are considered as the most vital factors in the operation. These factors have a significant influence on the power quality and efficiency of the system. Some parameters such as temperature, fluctuation of solar irradiance and semiconductor devices affect the power quality of PV which cause the variable power flow. As a result, voltage sag and voltage swell should be avoided in order to have a good power quality [25]. Figure 1.1 shows the general structure of grid-connected PV system [9].

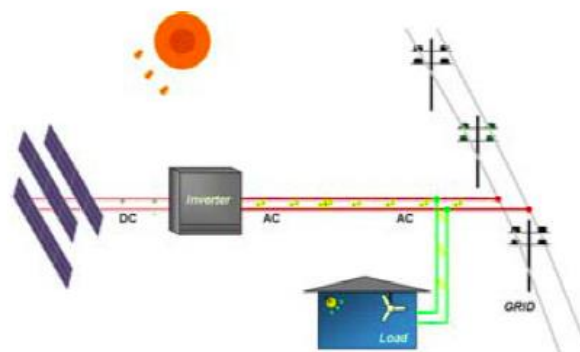


Figure 2.12: General structure of grid-connected PV system [9]

2.4.1 Steady State Voltage Variation

PV output power variations are caused by the variable nature of weather change, solar radiation or covering cloud. Figure 2.15 represents the variation of PV system power output during sunny day and cloudy day for 24 hours [26].

However, this project is intended to investigate the variation of PV system power output during the year by using Monte Carlo (MC) method.

According to [27], when the voltage and current are higher or lower than the normal limit, they can damage or shut down some types of electrical equipment. Studies presented in [28] suggested that super capacitor, which increases the cost of PV system around 20% can be the voltage and power mitigation.

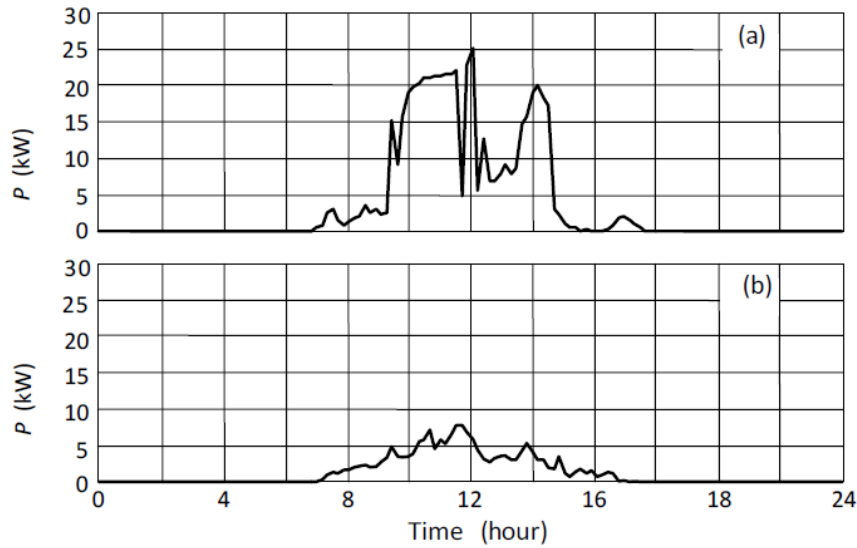


Figure 2.13: Variation of PV system power output during: (a) sunny day and (b) cloudy day [26]

As stated in [26], the voltage variation at point of common coupling (PCC) are expressed as following:

$$\Delta V = \frac{S_{pv}}{S_{sc}} \cdot \cos(\Psi_{sc} - \varphi) \quad (2.6)$$

where S_{sc} is the short circuit power at PCC, S_{pv} is the power produced by PV, φ is the phase angle of the PV output current, $\Psi_{sc} = \arctan(X/R)$ is the angle of the network short circuit impedance.

2.4.2 Distribution Transformer

Distribution transformer delivers the final voltage transformation from the primary feeder in the electric power distribution system to the secondary feeder by reducing the voltage for use in homes. It is usually center-tapped on the secondary side to provide voltages 120V/240V in residential homes as seen in Fig. 2.14. Integrating solar PV on the distribution transformers could be harmful for the system. Moreover, the impact of increasing the penetration of PV could result in distribution transformer overload, which exceeds the transformer rating or unbalance. Exceeding the rating of transformer results in reduced transformer life, damage to the winding and heating.

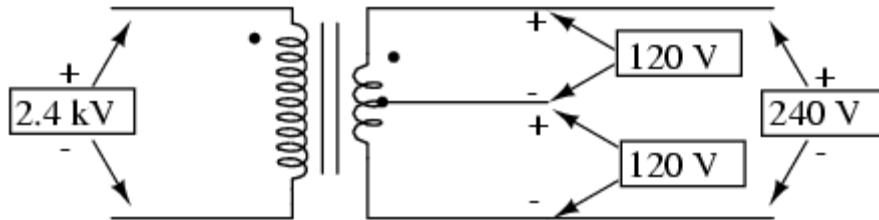


Figure 2.14: Center-tapped distribution transformer

2.5 Summary

This chapter presents a brief introduction to renewable energy explaining its concept along with the solar technologies. Solar characteristics and different modes of applications such as direct-coupled PV system, stand-alone application and grid-connected system are discussed in details. MicroFIT program that managed by the IESO is fleetingly explained in this chapter. Several voltage quality issues that are expected to occur during the integration of renewable energy are briefly highlighted and possible mitigations are presented. The following chapter will focus on Monte Carlo methods passing through the fundamentals and ends with the convergence issues.

CHAPTER 3

MONTE CARLO METHODS

3.1 Introduction

Monte Carlo methods are a class of algorithms that work by repeatedly sampling random points on the function domain [29]. These classes of algorithms are mainly used in optimization, numerical integration and generating a number from a give probability distribution. Monte Carlo methods are extremely useful for simulating physical systems which have different degrees of freedom. Example of such system would be fluids, disordered materials, cell structures, etc. They have applications in diverse fields such as calculation of risks in the field of finance, evaluating definite integrals of complicated boundary conditions, prediction of failures in space and oil explorations and cost overruns and schedule overruns in accounting and management [30].

3.2 Monte Carlo fundamentals

Monte Carlo (MC) means using random numbers as a tool to compute something that is not random. Let X be a random number and its expected value be $A=E[X]$. Therefore, if we generate independent random numbers $X_1, X_2 \dots X_n$ with same distribution then [31]:

$$A \approx \tilde{A} = 1/n * \sum X_k \quad (3.1)$$

Where $k = 1 \dots n$

The law of large numbers states that the average of results obtained from large numbers of trials is close to the expected mean. Thus the result would be closer to the mean if the numbers of trials are more. Hence $A \approx \tilde{A}$ as $n \rightarrow \infty$. Here X_k and \tilde{A} are random but the expected value A is not random.

The fact can be emphasized by distinguishing between Monte Carlo and simulation. Monte Carlo Simulation is a process of randomly generating inputs with a certain distribution in order to have an understanding of an output. For example we may be interested in the process of forming clouds by generating a simulation. However, to calculate the size of cloud or predicting if it would rain, we would move from simulation to Monte Carlo method [32].

Monte Carlo methods can be used to find the solution of integrals described by the expected value of some random variable by taking sample mean of independent samples of variable. When the probability distribution of variables is too complex then Markov chain Monte Carlo (MCMC) sampler is used. However, this method will not be considered in this project. There are other ways to estimate the expected value. They may be done by reducing the variance. As most of the error in \tilde{A} is statistical, reducing the variance would reduce the statistical error [32].

For finding a solution, random inputs are generated from the function domain and the results are computed for those inputs. The results are then aggregated to get the expected value. More the number of inputs, more precise are the result [33].

There is always a choice between Monte Carlo and deterministic methods. For a one dimensional random variable with a probability distribution function $f(x)$, the expected value may be estimated using panel integration. In this scenario the later would be more accurate than Monte Carlo methods. Monte Carlo methods would give a large error, for large numbers as the error is proportional to $1/\sqrt{n}$ [32].

3.3 Monte Carlo simulation

Electrical mismatch issue for large scale photovoltaic array has to be addressed to minimize the losses. For this, the photovoltaic arrays are divided into current or voltage classes. These arrays are then connected in series or in parallel connection according to the class they belong to. If it is a series connection then it would belong to the current class, and if it is connected in parallel then it would belong to the voltage class. Since a lot of time and array modules are required, this process is not effective in predicting the electrical mismatch losses. In the above process, the electrical mismatch loss is either calculated by analyzing the overall circuit of the photovoltaic generator, starting from the electrical parameters (I_{sc} & V_{oc}) of the single photo voltaic array module or by randomly arranging the photovoltaic modules and defining their electrical parameters through a probability distribution function. The later case is called the statistical circuit synthesis of the photovoltaic generator [30-32].

Many works have been reported in the literature to analyze the effect of input parameters on electrical mismatch. In [30 & 34], a sensitivity analysis was employed to evaluate the effect of input parameters on electrical mismatch in small scale generators. In addition, [35] randomly

generates solar cell modules to analyze the voltage current characteristics. In [36], a mathematical formulation was introduced to statistically analyze mismatch.

The study in [34] describes the model of single photovoltaic cell voltage current characteristics in forward and reverse bias conditions. Figure 3.1 shows the equivalent model of the photovoltaic cell [30].

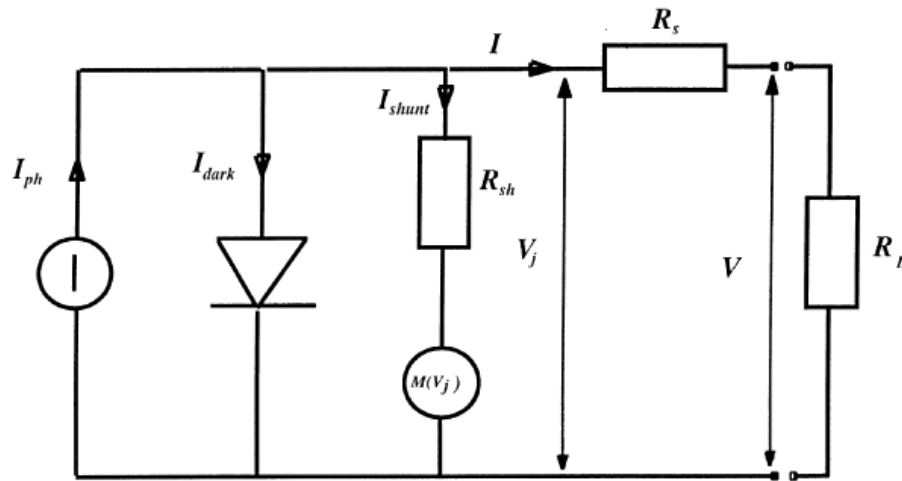


Figure 3.1: Equivalent circuit of the PV module [30]

Where,

R_{sh} = Shunt resistor,

R_s = Series resistor,

I_{sh} = Leakage current,

$M(V_j)$ = Nonlinear factor to take into account breakdown voltage,

I_{ph} = Photo current,

I_o = Saturation Current.

The analytical model of the system is given below

$$I = I_{ph} - I_o \left(e^{\frac{V+R_s I}{\eta V_T}} - 1 \right) - I_{sh} \quad (3.2)$$

$$I_{sh} = \frac{V+R_s I}{R_{sh}} \cdot \left[1 + a \cdot \left(1 - \frac{V+R_s I}{V_{br}} \right)^{-m} \right] \quad (3.3)$$

I_o and I_{ph} depend on the series and shunt resistance through equations:

$$\begin{aligned} I_o = & \{ I_{sc} - V_{oc}/R_{sh} [1 + a(1 - V_{oc}/V_{br})^{-m}] \\ & + R_s \cdot I_{sc}/R_{sh} [1 + a(1 - R_s \cdot I_{sc}/V_{br})^{-m}] \} \\ & / \{ \exp [V_{oc}/(\eta V_{oc})] - \exp [R_s \cdot I_{sc}/(\eta V_{oc})] \} \end{aligned} \quad (3.4)$$

And

$$\begin{aligned} I_{ph} = & I_o \{ \exp [V_{oc}/(\eta V_T)] - 1 \} \\ & + \frac{V_{oc}}{R_{sh}} \left[1 + a \left(1 - \frac{V_{oc}}{V_{br}} \right)^{-m} \right]. \end{aligned} \quad (3.5)$$

The standard test conditions of photovoltaic cell is at an irradiance of 1000 Watt per meter squared at a temperature of 25 degree Celsius. To modify this we adapt the initial conditions to the equations given below [30]:

$$I_{sc} = \tilde{I}_{sc} + \Delta I_{sc} \quad (3.6)$$

$$V_{oc} = \tilde{V}_{oc} - \beta(T - 25^\circ) - R_s \Delta I_{sc} - K(T - 25^\circ) I_{sc} \quad (3.7)$$

$$\Delta I_{sc} - \tilde{I}_{sc} \left(\frac{\phi}{1000} - 1 \right) + \alpha(T - 25^\circ) \quad (3.8)$$

Where V_{oc} and I_{sc} are the open circuit voltage and the short circuit current at standard test conditions, α and β are thermal correction parameters, K is the shape correction parameter, ϕ and T are actual values of irradiance and temperature respectively.

As mentioned earlier, modules population can be defined using Monte Carlo method by assuming the electrical parameters as random variable having a probability distribution. Here I_{sc} and V_{oc} are the electrical parameters and Gaussian probability distribution is used to analyze data when there is an equally likely chance of being above or below the mean for continuous data. We get the following equations [30]:

$$X \sim N(\langle x \rangle, \sigma) \Leftrightarrow f_X = (2\pi\sigma^2)^{-1/2} \times \exp[-(x - \langle x \rangle)^2 / (2\sigma^2)]. \quad (3.9)$$

Where $\langle x \rangle$ is the Gaussian moment of I_{sc} and σ is the Gaussian moment of V_{oc}

3.4 Convergence issues

We can use the above mentioned parameters to evaluate the maximum power directly. To generate the random population of inputs, the probability density functions Gaussian moments are set to 0 and 1 for I_{sc} and V_{oc} respectively. We can calculate the other parameters of the V-I curve using Monte Carlo analysis like Voltage, current, maximum voltage and maximum current. The

probability density function of the derived variable will be similar to the probably density function of the input variable I_{sc} and V_{oc} with similar standard deviation and the mean. Hence we can satisfactorily assume the correctness of Monte Caro Method [31]. Figure 3.2 shows the Monte Carlo technique being applied to find the value of pi. It can be seen that the Value converges to the expected value after a large number of runs, here it is ten thousand.

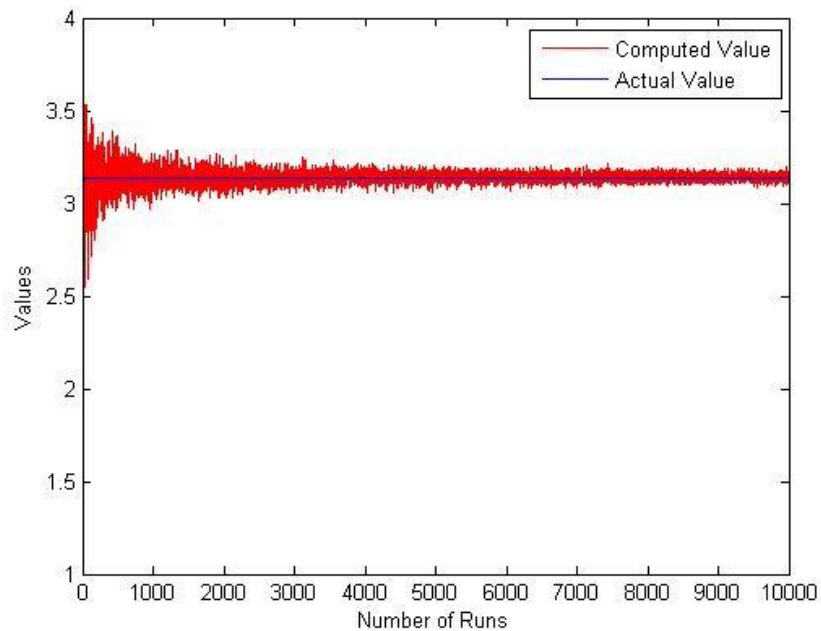


Figure 3.2: Value converges by using Monte Carlo technique.

3.5 Summary

The chapter discussed the simulation of Monte Carlo method and its application to PV. The chapter also presented the model of single photovoltaic cell voltage current characteristics in details. Furthermore, the convergence issue by using Monte Carlo technique is highlighted.

CHAPTER 4

SIMULATION & RESULTS

4.1 Introduction

This chapter includes six scenarios simulated by Monte Carlo (MC) Method. This method has an advantage to address the uncertainties which causing by temperature and solar irradiance in case of solar photovoltaic. The PVs installed on the rooftop of each house are ranging from 0 kW (no PV) to 10 kW (maximum solar PV capacity per house according to [37]) [38].

The scenarios presented in this chapter will take into account the solar irradiance (W/m²) and temperature (Degree Celsius) data in Toronto which are collected from Canadian Weather Energy Engineering Datasets (CWEED) [39]. The weather stations in Ontario are obtained from the folder labeled “ONTARIO.zip”.

The results from the study will present the objective of this work which can be summarized in two points: 1) the effect of PVs on the house voltage and 2) the transformer’s power. Moreover, the Loss of Life (LOL) for both 25 and 50 KVA transformers are calculated. As stated in [40], the minimum life expectancy for transformers is 180 000 hours, while the normal percent LOL for operation is 0.0133% for 24 hours.

4.2 Primary Distribution System

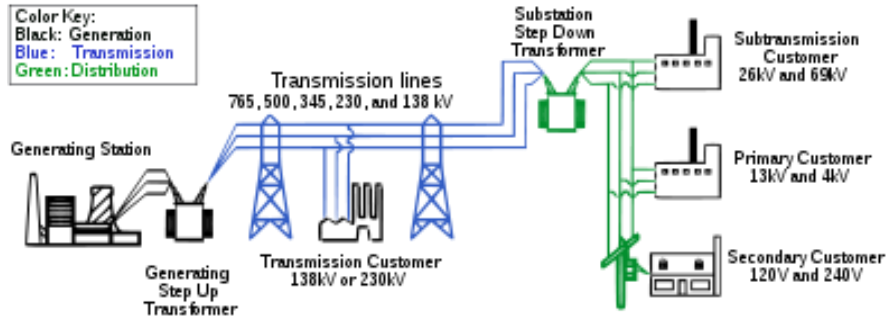


Figure 4.1 Power generation, transmission and distribution

The primary distribution systems generally begin from the distribution substations and end at the distribution transformers as seen in Fig. 4.1 and 4.2. The primary distribution systems contain main feeders and lateral feeders. Transmission lines commonly deliver electric power from power plants to substations over long distances and conduct 69 kilovolts (kV) or more. However, distribution lines deliver electric power to commercial and residential customers from substations and conduct less than 69 kV.

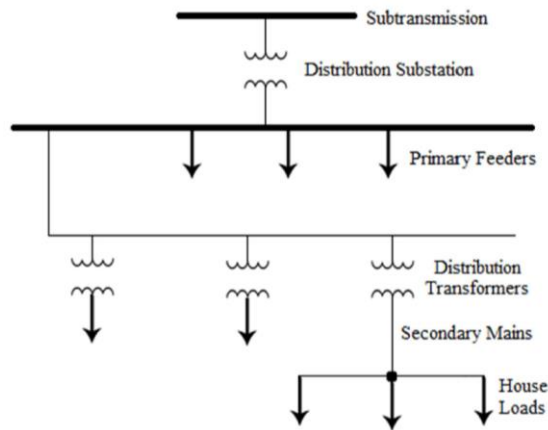


Figure 4.2: Generalized Distribution System

4.3 Secondary Distribution System

The secondary distribution systems start from the distribution transformers as shown in Fig. 4.2. The distribution transformers step down the primary voltage to 120/240 voltage in order to suit the consumers' equipment. In this project, two transformer sizes are chosen, 25 kVA and 50 kVA, and two archetypes that support 6 and 10 houses as seen in Fig. 4.3 and 4.4 are used to connect the residential house loads on the secondary system.

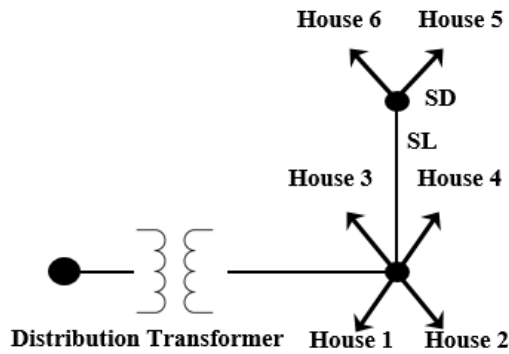


Figure 4.3: A 25 kVA Distribution Transformer with 6 Houses

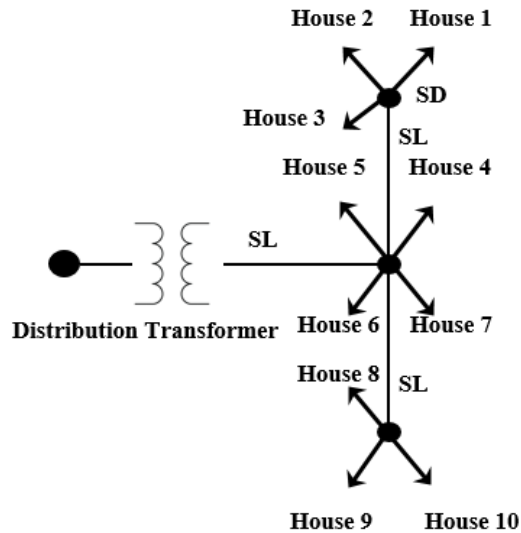


Figure 4.4: A 50 kVA Distribution Transformer with 10 Houses

4.4 System Description

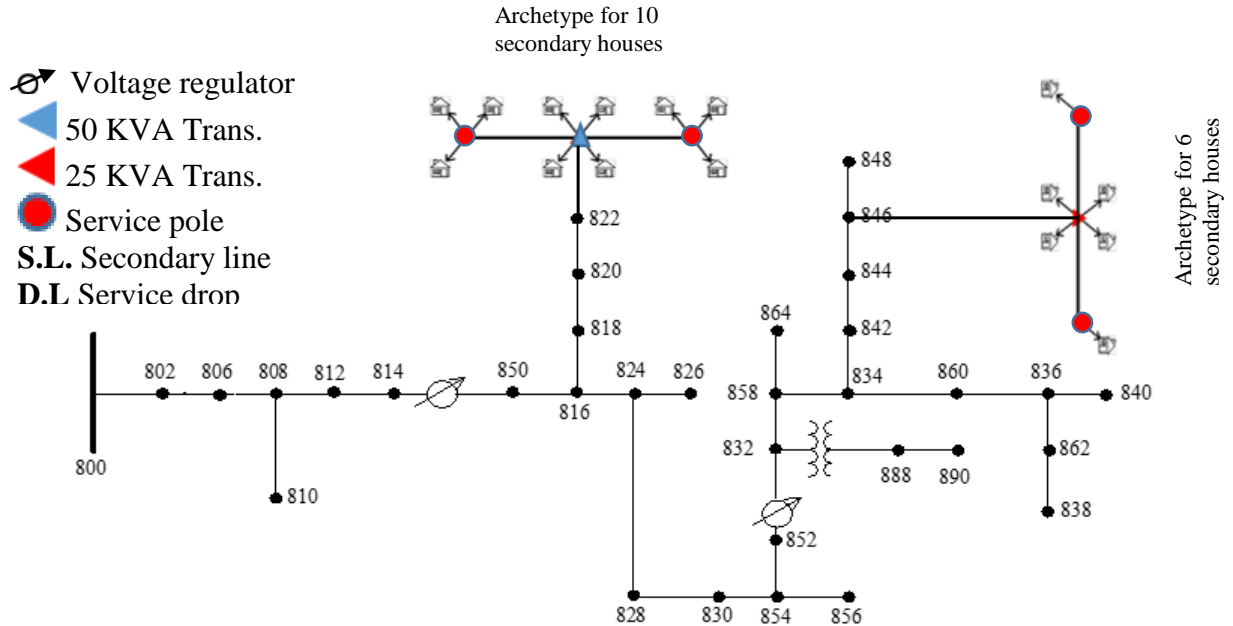


Figure 4.5: Modified IEEE 34-Bus Standard Test System [41]

The IEEE Power and Energy Society (PES) website provides benchmark test distribution systems of different sizes such as 13, 34 or 123 Bus Test Feeders. The IEEE 34 Bus Standard Test Distribution System [41] is chosen after carefully examining the published test systems. The system is modified by extending the secondary system and modelling the distribution transformers, secondary service lines (SLs) and service drops (SDs) using Open-DSS [42]. The spot loads on the primary system are replaced by distribution transformers, service lines (length=125 feet) and service drops (length= between 80-100 feet) feeding residential homes. Figure 4.5 shows the modified IEEE 34-Bus Standard Test System after adding the secondary circuit. The data of the IEEE 34-Bus Standard Test System is outlined in Appendix A. A sample secondary, showing a 50 kVA and 25 kVA transformers configurations at nodes 822 and 846 supplying 10 houses and 6 houses respectively, are shown in Fig. 4.5.

In this work, two transformer sizes are chosen, 25 kVA and 50 kVA, and two archetypes that support 6 and 10 houses as seen in Fig. 4.3 and 4.4 are used to connect the residential house loads on the secondary system. The choice of transformer sizes and archetypes are to match the equivalent spot load on the primary. For example, spot loads with peak value 44.72 kVA are replaced by 10 residential homes and supplied by 50 kVA distribution transformer [38]. The archetypes shown in Fig. 4.3 and 4.4 are to support 6 and 10 houses and in this case a 25 kVA and 50 KVA transformers is chosen to feed these six and ten houses respectively.

The data of the secondary system extension including the distribution transformers is in Appendix B. The rooftop solar PV considering different scenarios (6 scenarios), vary from 0 kW to 10 kW and simulated using Monte Carlo.

4.5 System Data

4.5.1 Temperature

Solar irradiance (W/m²) and temperature (Degree Celsius) data in Toronto are collected from Canadian Weather Energy Engineering Datasets (CWEED) as seen in Table 4.1 and Figure 4.6.

Month	Temperature
January	-5.0167
February	-6.0292
March	-1.4208
April	10.1
May	15.175
June	22.458
July	24.292
August	21.7
September	21.488
October	11.313
November	4.125
December	-0.0125

Table 4.1: Toronto Temperature Data

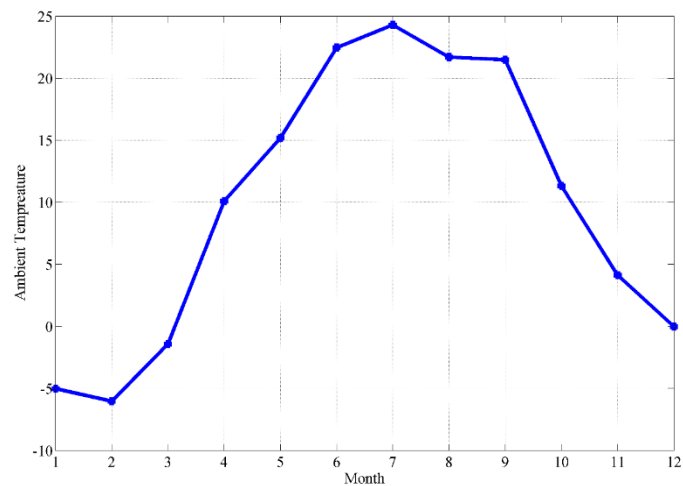


Figure 4.6: Monthly Temperature in Toronto, Canada

4.5.2 Transformer

There are two center tapped distribution transformers for the system (25 kVA & 50 kVA) and the parameters are listed in Table 4.2 [43].

Transformer	KVA	KV- high	KV- low	R - %	X - %
Secondary 25KVA	25	4.16 - D	0.24 Gr-W	0.5367	1.0733
Secondary 50KVA	50	4.16 - D	0.24 - D	1.0140	1.7239

Table 4.2: Center Tapped Distribution Transformer Parameters [43]

4.6 Applying Monte Carlo Method (MC)

The Monte Carlo algorithm is used to compute the impact of irradiance and temperature on the output voltage of PVs and considering the 6 scenarios listed in Table 4.1. The steps of implementing the MC algorithm to the modified IEEE 34-bus including the secondary circuits and the power generated from solar PV. The number of runs “trials” for MC is set from 1000 to 5000 for each PV at 0, 2, 4, 6, 8 and 10 kW/home. The secondary system results will consider only the 5000 trial for each scenario as an example for the rest trials.

Case Number	Trial	PV (kw/home)
Scenario#1	1000	0
	2000	
	3000	
	4000	
	5000	
Scenario#2	1000	2
	2000	
	3000	
	4000	
	5000	
Scenario#3	1000	4
	2000	
	3000	
	4000	
	5000	
Scenario#4	1000	6
	2000	
	3000	
	4000	
	5000	
Scenario#5	1000	8
	2000	
	3000	
	4000	
	5000	
Scenario#6	1000	10
	2000	
	3000	
	4000	
	5000	

Table 4.3: Modified IEEE 34-Bus Standard Test System

4.7 Secondary System Results

Figure 4.7 shows the variation of PV system output power in the scenarios considered. It can be easily seen when the transformer rate is 50 kVA, the variation of PVs from 0 to 10 kW has no noticed effect on the house voltage, except the time between 11-15h which shows very little effect range between 119-119.6V. All scenarios are drawn in one figure to clearly see the differences of house voltages with applying different PV penetrations.

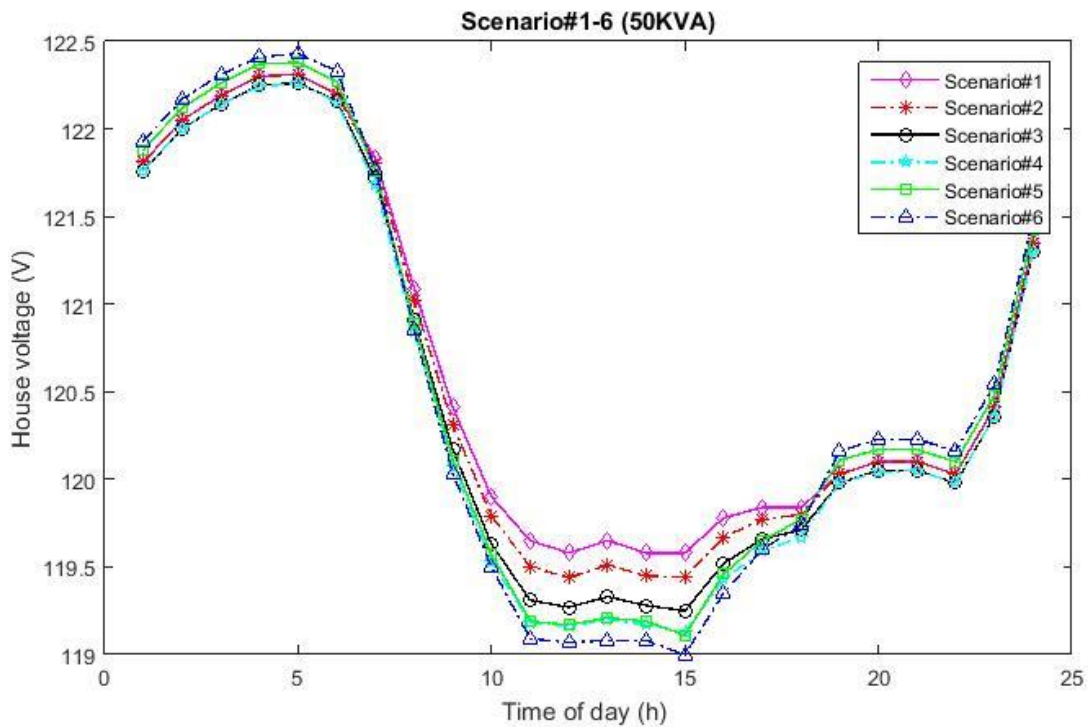


Figure 4.7: Variation of PV system power output during applying different scenarios & 50KVA

The voltage of the house supplied from 25 kVA transformer seems to be affected more compared to that connected top 50 kVA transformer when applying different PVs rates as seen in Figure 4.8. The variation is between the hours 6 and 19 and range from 112.3 to 123V. It is also

noticed that when the PV rate increases, the variation of the house voltage increases. Therefore, the variation of house voltage (V) is proportional to the PV rates.

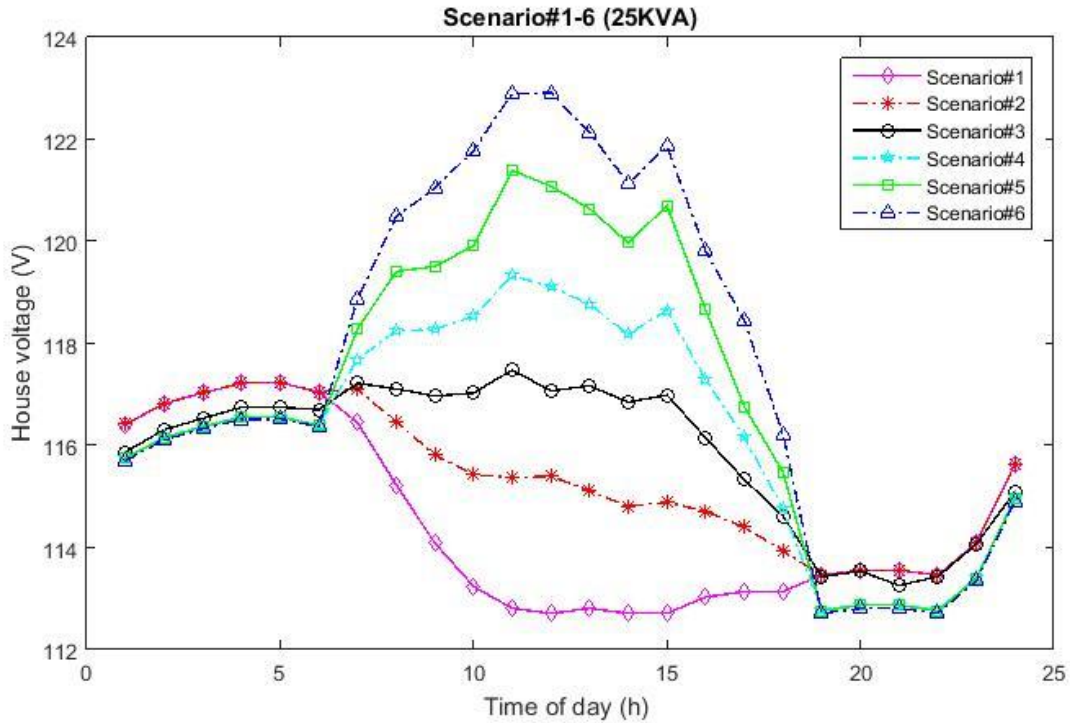


Figure 4.8: Variation of PV system power output during different scenarios & 25KVA

Table 4.4 below lists the transformer loading. It shows the optimal transformer rating, number of customers, service drop and secondary line for each extension bus.

Extension Bus	Best Transformer Rating	Extension Phase	Best Number of Customer	Best number of Right branch	Best number of Left branch	Best SDs	Best SLs	
822	50	1	10	1	1	106.5	106.5	0
846	25	2	6	1	1	106.5	106.5	0

Table 4.4: Transformer Loading

4.7.1 Scenario#1

4.7.1.1 Convergence

The convergence plot allows to determine whether or not the analysis results are converging to constant values through viewing the progress of a probabilistic analysis, and it also allows to determine the approximate number of samples at which convergence occurs which can help to decide if you have used enough samples for the probabilistic analysis, or if you can use fewer samples, and still obtain valid results.

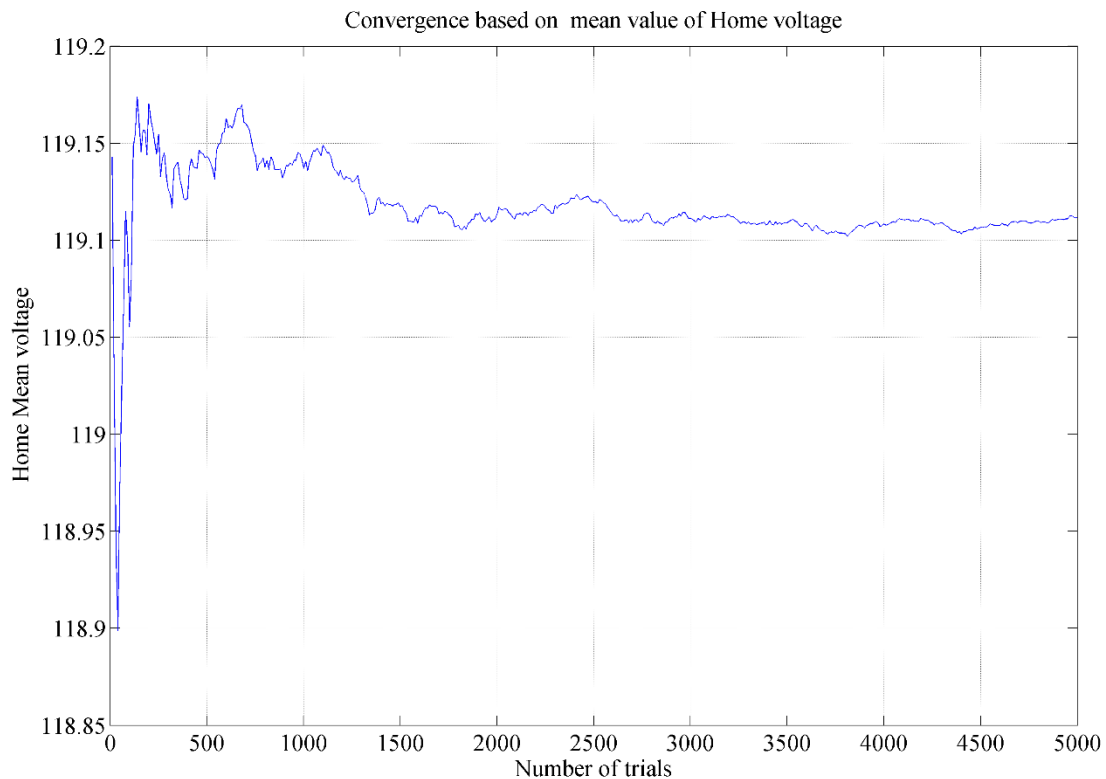


Figure 4.9: Convergence based on mean value of home voltage

Figure 4.9 above shows the convergence based on mean value of home voltage. It can be seen that the value of home voltage (Secnario#1) is fluctuating between 0 and 1200 trials. However, at 1300 trials, the value of home voltage converges and remains stable until 5000 trials.

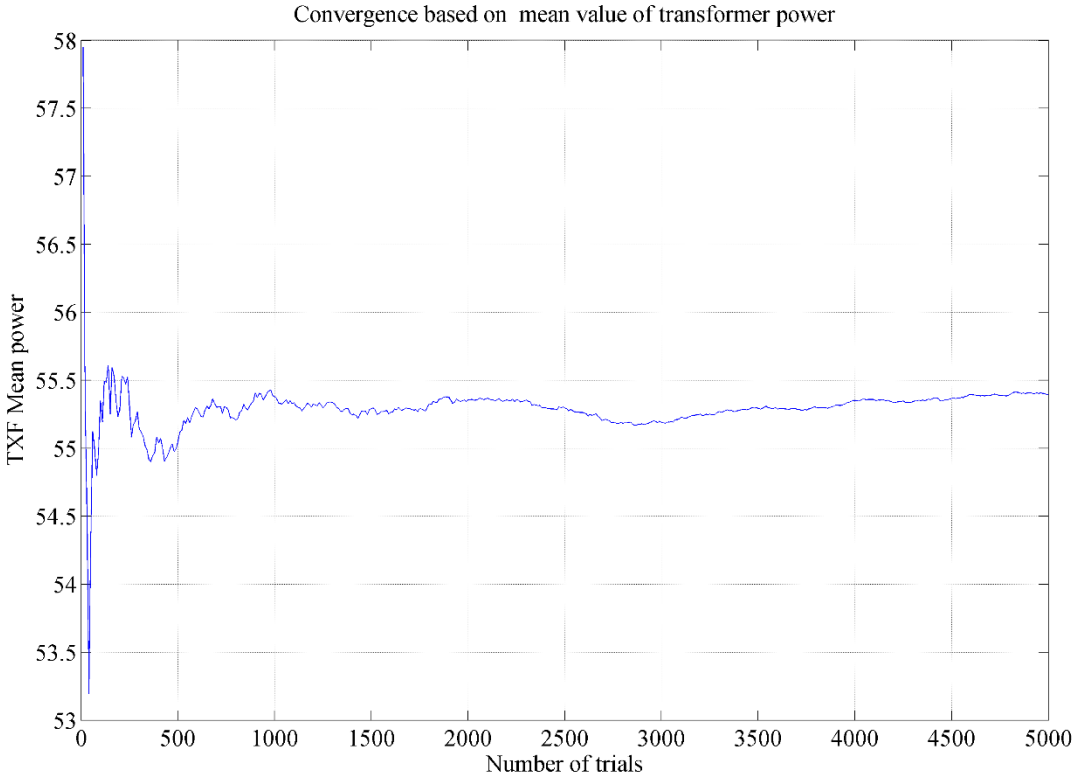


Figure 4.10: Convergence based on mean value of transformer power

Figure 4.10 depicts the convergence based on mean value of transformer power. Based on the figure, the value of transformer power (Secnario#1) at 700 trials is believed to be the convergence point, and the value remains almost constant towards the 5000 trials.

4.7.1.2 Loss of Life

Month	50 kVA Transformer	25 kVA Transformer	Temperature
January	0.000167	0.000152	-5.0167
February	8.65E-05	7.85E-05	-6.0292
March	1.27E-05	1.02E-05	-1.4208
April	0.00017	0.000133	10.1
May	0.001764	0.001601	15.175
June	0.00528	0.004907	22.458
July	0.00209	0.001864	24.292
August	0.000762	0.0006	21.7
September	0.000436	0.000321	21.488
October	0.000183	0.000143	11.313
November	0.001075	0.000993	4.125
December	0.001182	0.001104	-0.0125

Table 4.5: Transformer Loss of Life during the year

Table 4.5 lists the Loss of Life in 25 kVA and 50 kVA during one year. The results are in percent, and it shows monthly LOL for each transformer. It can be seen that the monthly LOL of the 25 kVA transformer is less compared to that of the 50 kVA transformer due to no load (PV=0). Therefore, the total yearly LOL (50 kVA & 25 kVA) would be 0.40225% and 0.362491% respectively. The calculation of the transformer insulation life is outlined in Appendix C.

4.7.2 Scenario#2

4.7.2.1 Convergence

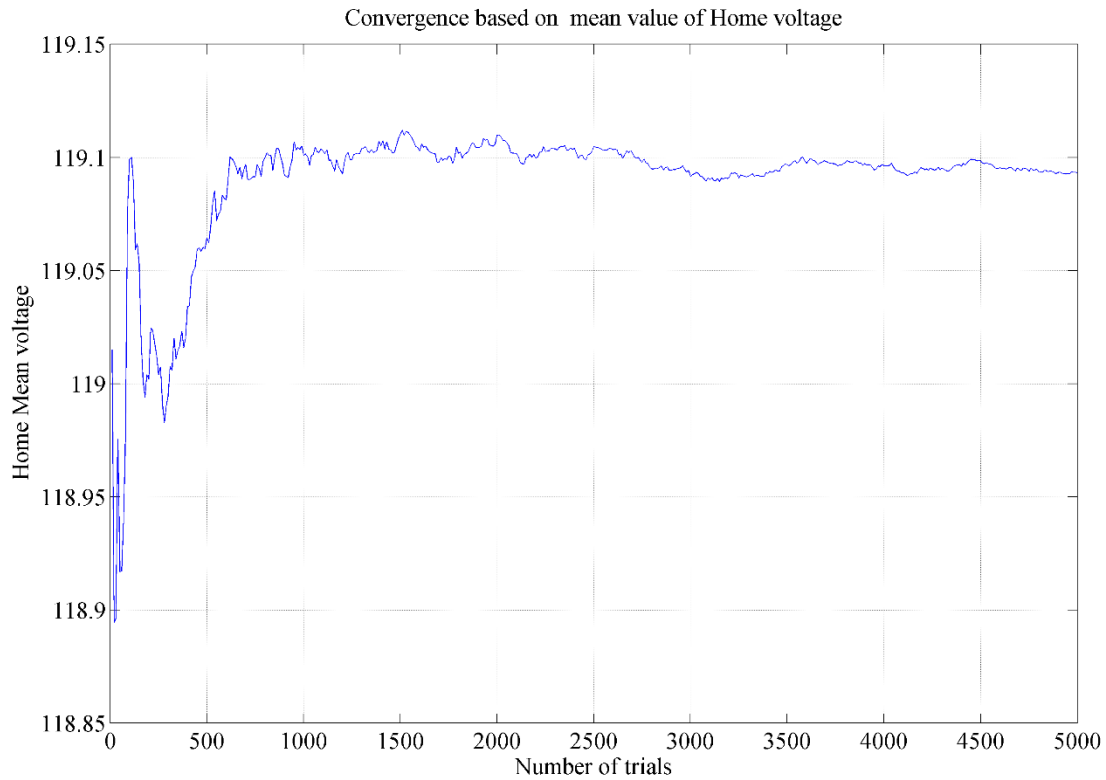


Figure 4.11: Convergence based on mean value of home voltage

Figure 4.11 expresses the convergence based on mean value of home voltage. The value of home voltage (Scenario#2) is not stable between 0 and 500 trials. However, at 600 trials, the value of home voltage converges and remains almost steady until 5000 trials.

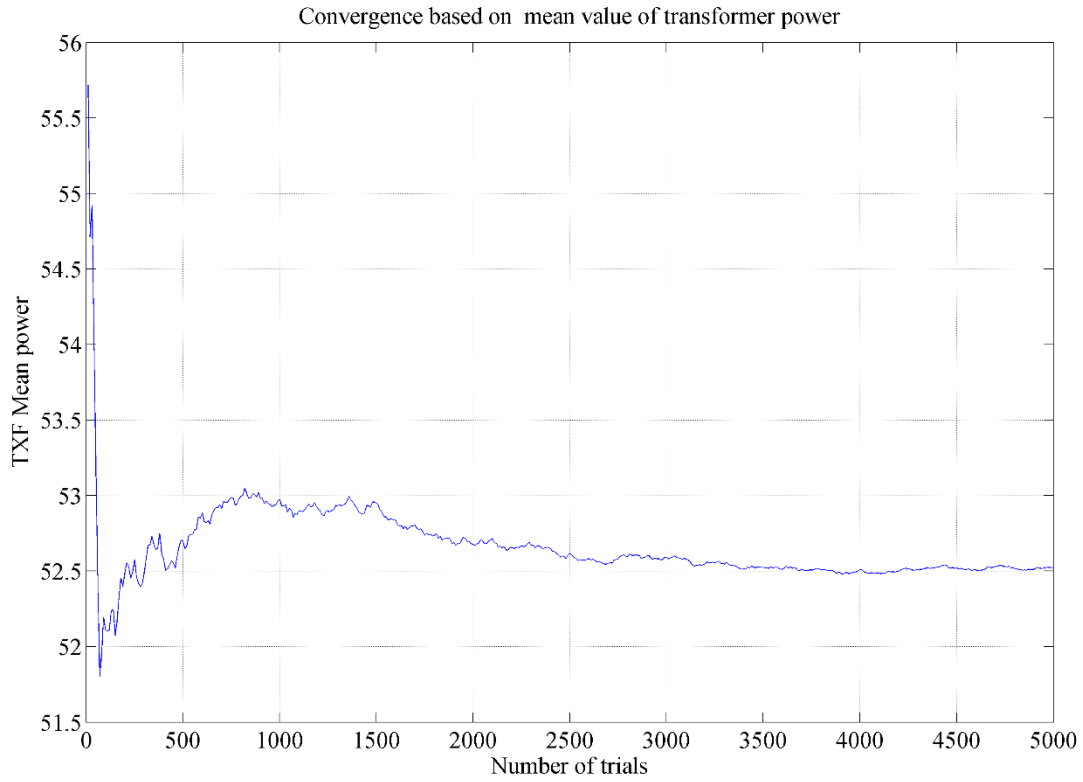


Figure 4.12: Convergence based on mean value of transformer power

Figure 4.12 shows the convergence based on mean value of transformer power. It is seen that the value of transformer power (Secnario#2) at 2500 trials is the convergence point, and the value remains stable towards the 5000 trials.

4.7.2.2 Loss of Life

Month	50 kVA Transformer	25 kVA Transformer	Temperature
January	8.39E-05	0.00015	-5.0167
February	4.09E-05	7.47E-05	-6.0292
March	6.3E-06	1.08E-05	-1.4208
April	6.33E-05	0.000133	10.1
May	0.000391	0.001607	15.175
June	0.001507	0.004949	22.458
July	0.000817	0.001875	24.292
August	0.000251	0.000602	21.7
September	0.000176	0.000323	21.488
October	9.63E-05	0.000142	11.313
November	0.000832	0.000988	4.125
December	0.001052	0.001097	-1.8708

Table 4.6: Transformer Loss of Life during the year

Table 4.6 lists the Loss of Life in 25 kVA and 50 kVA during one year. It can be observed that the monthly LOL of the 25 kVA transformer is much greater than the 50 kVA transformer. Therefore, the total yearly LOL of 50 kVA and 25 kVA are 0.162119% and 0.36386% respectively.

4.7.3 Scenario#3

4.7.3.1 Convergence

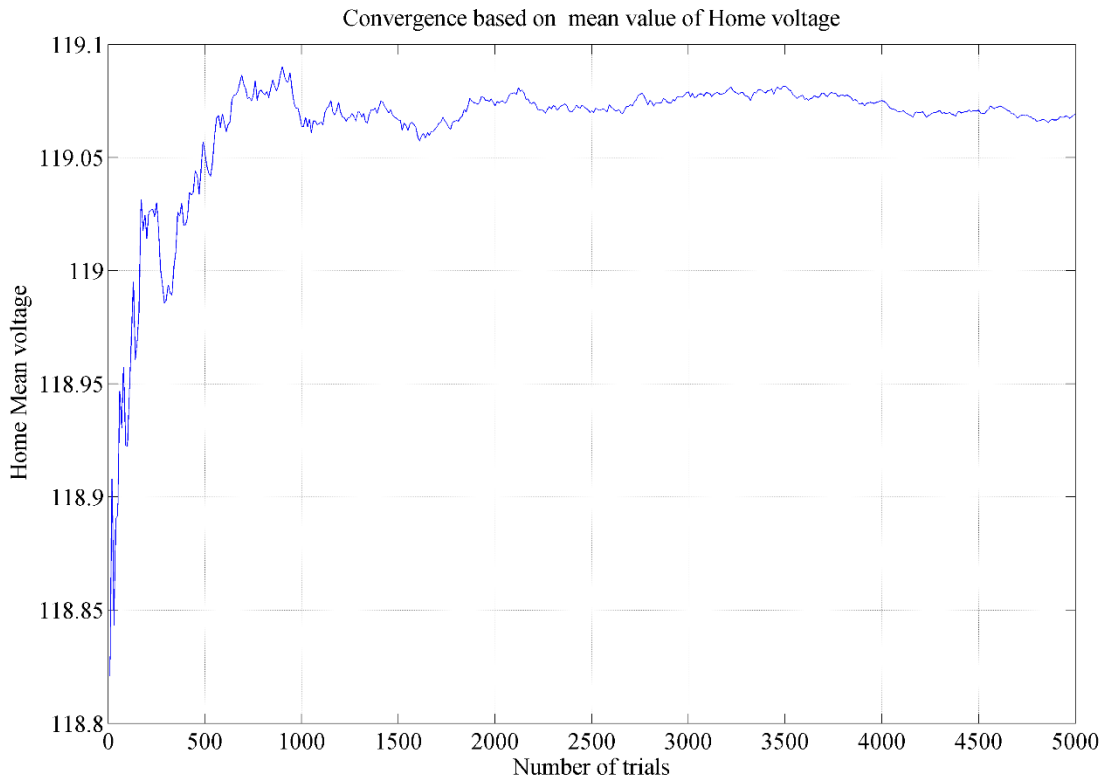


Figure 4.13: Convergence based on mean value of home voltage

Figure 4.13 illustrates the convergence based on mean value of home voltage. The value of home voltage (Scenario#3) is fluctuating between 0 and 900 trials. However, at 1000 trials, the value of home voltage converges and remains almost steady until 5000 trials.

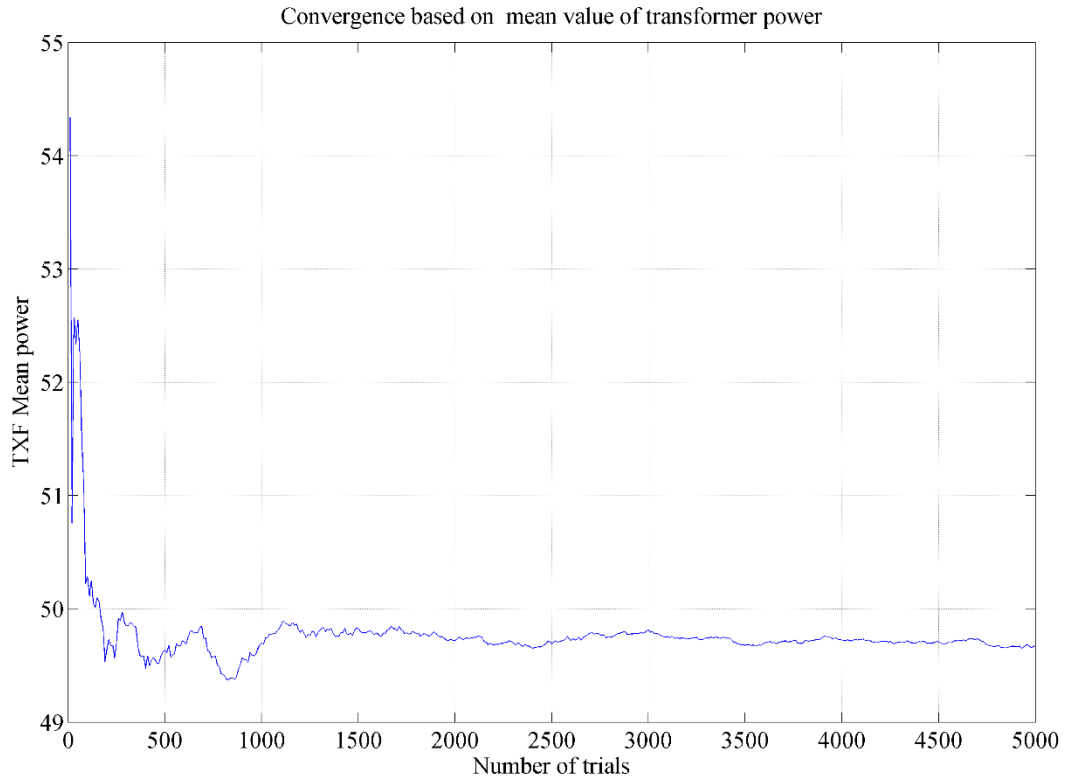


Figure 4.14: Convergence based on mean value of transformer power

Figure 4.14 depicts the convergence based on mean value of transformer power. Based on the above figure, the value of transformer power (Secnario#3) at 1100 trials is believed to be the convergence point, and the value remains constant until the 5000 trials.

4.7.3.2 Loss of Life

Month	50 kVA Transformer	25 kVA Transformer	Temperature
January	5.14E-05	0.00015	-5.0167
February	2.41E-05	7.76E-05	-6.0292
March	5.19E-06	1.01E-05	-1.4208
April	3.51E-05	0.000135	10.1
May	0.000207	0.001585	15.175
June	0.000685	0.004833	22.458
July	0.000411	0.001881	24.292
August	0.00014	0.000597	21.7
September	0.000105	0.000319	21.488
October	5.8E-05	0.000141	11.313
November	0.000543	0.000992	4.125
December	0.000933	0.001072	-0.0125

Table 4.7: Transformer Loss of Life during the year

Table 4.7 lists the Loss of Life in 25 kVA and 50 kVA during one year. The above results (in percent) describe the monthly LOL of both transformers. The monthly LOL of the 25 kVA is much greater than the 50 kVA transformer. As a result, the total yearly LOL of 50 kVA and 25 kVA are 0.097681% and 0.359053% respectively.

4.7.4 Scenario#4

4.7.4.1 Convergence

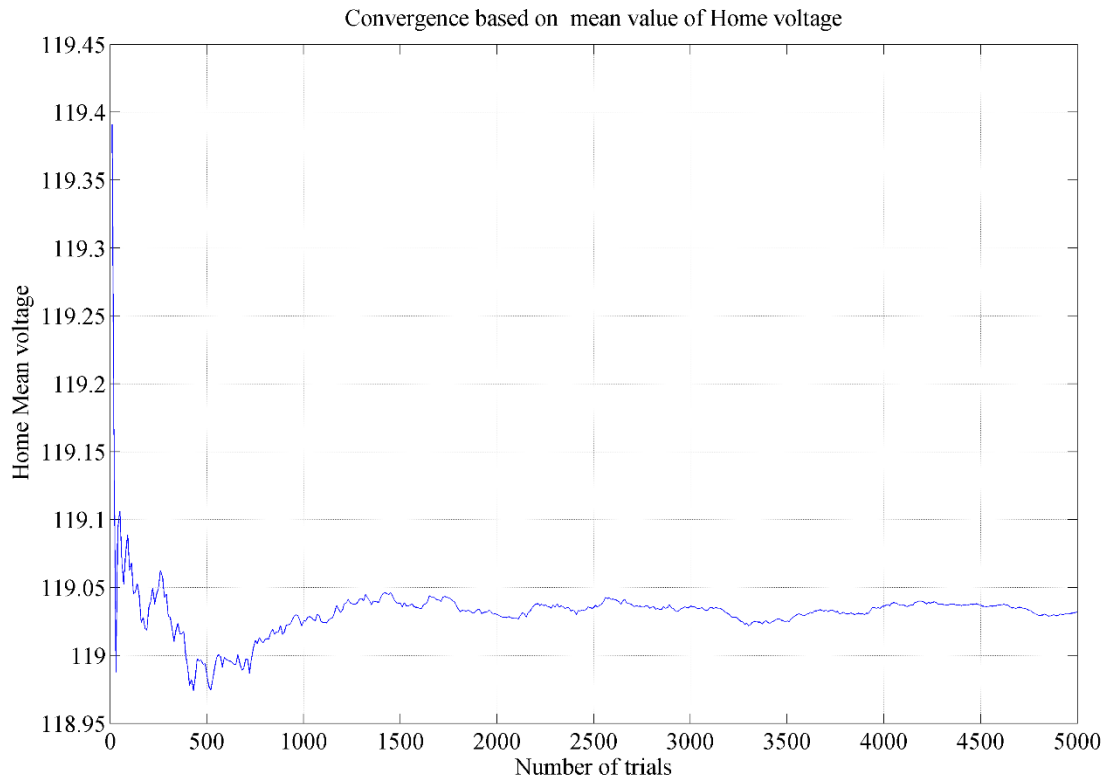


Figure 4.15: Convergence based on mean value of home voltage

The above Figure 4.15 shows the convergence based on mean value of home voltage. The value of home voltage (Scenario#4) is fluctuated between 0 and 1000 trials. However, at 1100 trials, the value of home voltage converges and remains almost steady until 5000 trials.

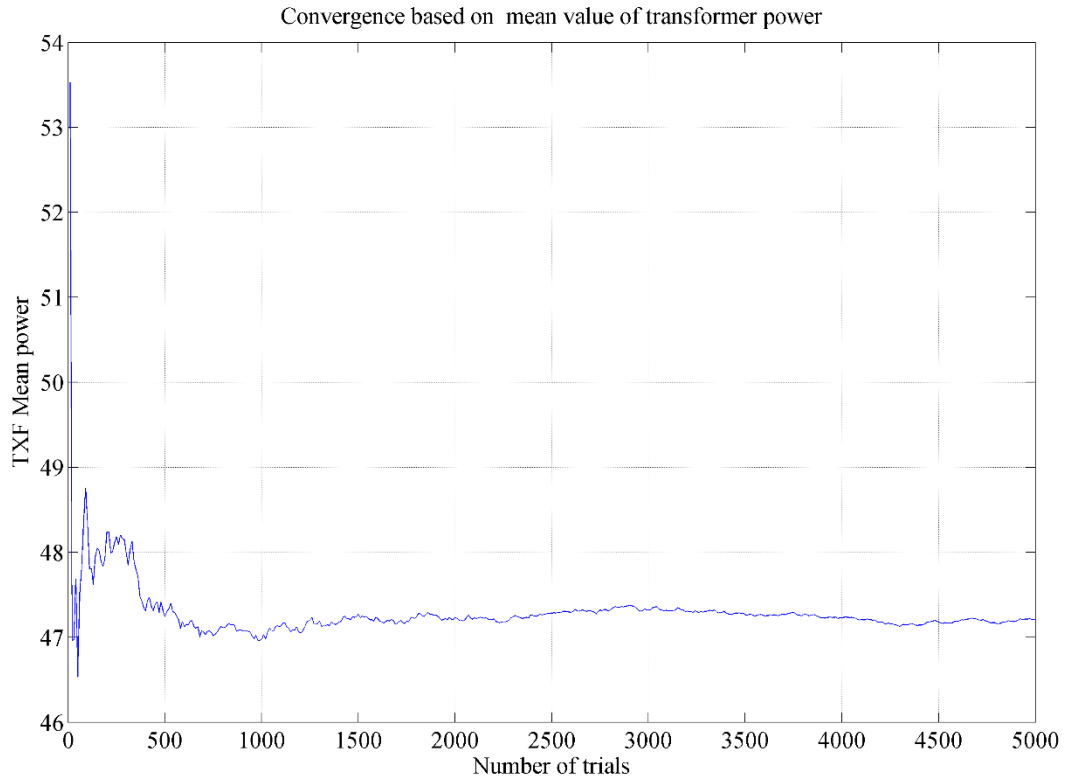


Figure 4.16: Convergence based on mean value of transformer power

Figure 4.16 illustrates the convergence based on mean value of transformer power. It is seen that the value of transformer power (Secnario#4) at 600 trials is the convergence point, and the value remains stable towards the 5000 trials.

4.7.4.2 Loss of Life

Month	50 kVA Transformer	25 kVA Transformer	Temperature
January	3.23E-05	0.00015	-5.0167
February	1.66E-05	7.59E-05	-6.0292
March	4.19E-06	1E-05	-1.4208
April	2.96E-05	0.000131	10.1
May	0.000134	0.001601	15.175
June	0.000464	0.004922	22.458
July	0.000298	0.001872	24.292
August	0.000103	0.000606	21.7
September	8.44E-05	0.000324	21.488
October	4.32E-05	0.000143	11.313
November	0.000447	0.000991	4.125
December	0.000821	0.001078	-0.0125

Table 4.8: Transformer Loss of Life during the year

Table 4.8 lists the Loss of Life in 25 kVA and 50 kVA during one year. The results (in percent) shows that the monthly LOL of the 25KVA is much greater than the 50KVA transformer. Consequently, the total yearly LOL of 50KVA and 25KVA are 0.075718% and 0.362365% respectively.

4.7.5 Scenario#5

4.7.5.1 Convergence

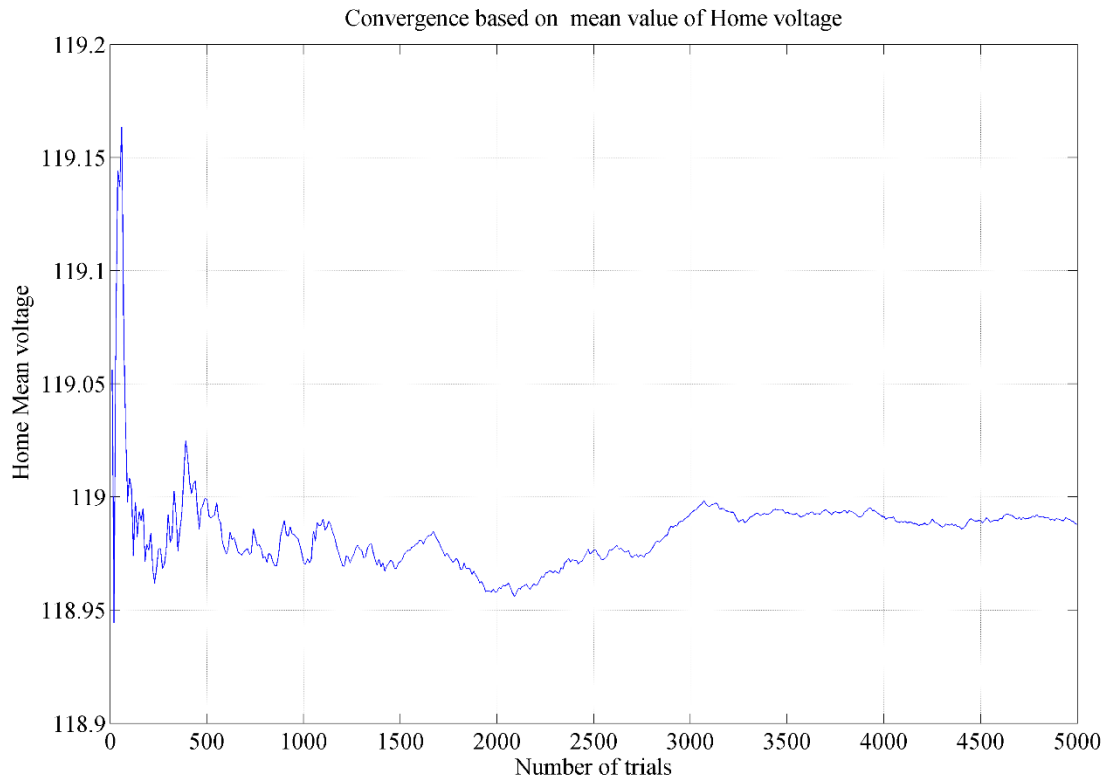


Figure 4.17: Convergence based on mean value of home voltage

Figure 4.17 shows the convergence based on mean value of home voltage. It can be seen that the value of home voltage (Scenario#5) is fluctuating between 0 and 400 trials. However, at 500 trials, the value of home voltage converges and remains almost stable until 5000 trials.

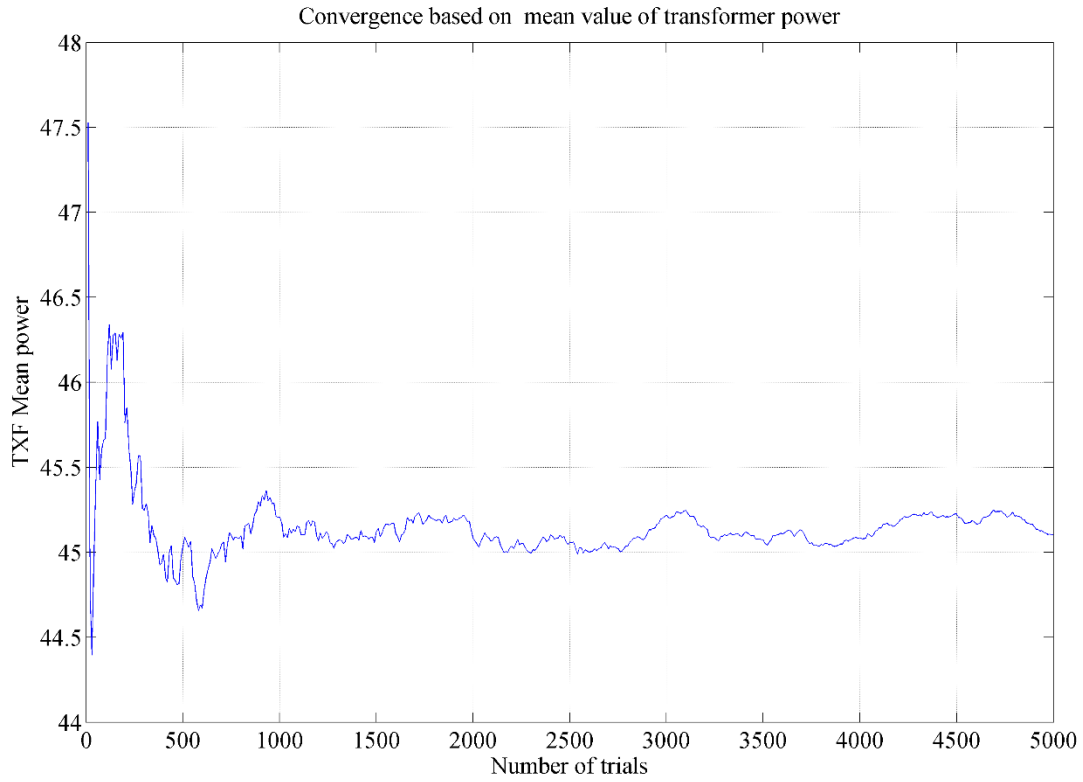


Figure 4.18: Convergence based on mean value of transformer power

The above Figure 4.18 demonstrates the convergence based on mean value of transformer power. Based on the figure, the value of transformer power (Secnario#5) at 700 trials is believed to be the convergence point, and the value remains almost constant towards the 5000 trials.

4.7.5.2 Loss of Life

Month	50 kVA Transformer	25 kVA Transformer	Temperature
January	2.42E-05	0.000151	-5.0167
February	1.37E-05	7.55E-05	-6.0292
March	3.99E-06	1.03E-05	-1.4208
April	3.88E-05	0.000133	10.1
May	0.000129	0.001604	15.175
June	0.000413	0.004855	22.458
July	0.000323	0.001876	24.292
August	0.000123	0.000598	21.7
September	9.32E-05	0.000323	21.488
October	3.88E-05	0.000141	11.313
November	0.000412	0.000991	4.125
December	0.000701	0.001122	-0.0125

Table 4.9: Transformer Loss of Life during the year

Table 4.9 lists the Loss of Life in 25 kVA and 50 kVA during one year. It can be seen from the above results (in percent) that the monthly LOL of the 25 kVA transformer is far greater than the 50 kVA transformer. Accordingly, the total yearly LOL of 50 kVA and 25 kVA are 0.070741% and 0.36173% respectively.

4.7.6 Scenario#6

4.7.6.1 Convergence

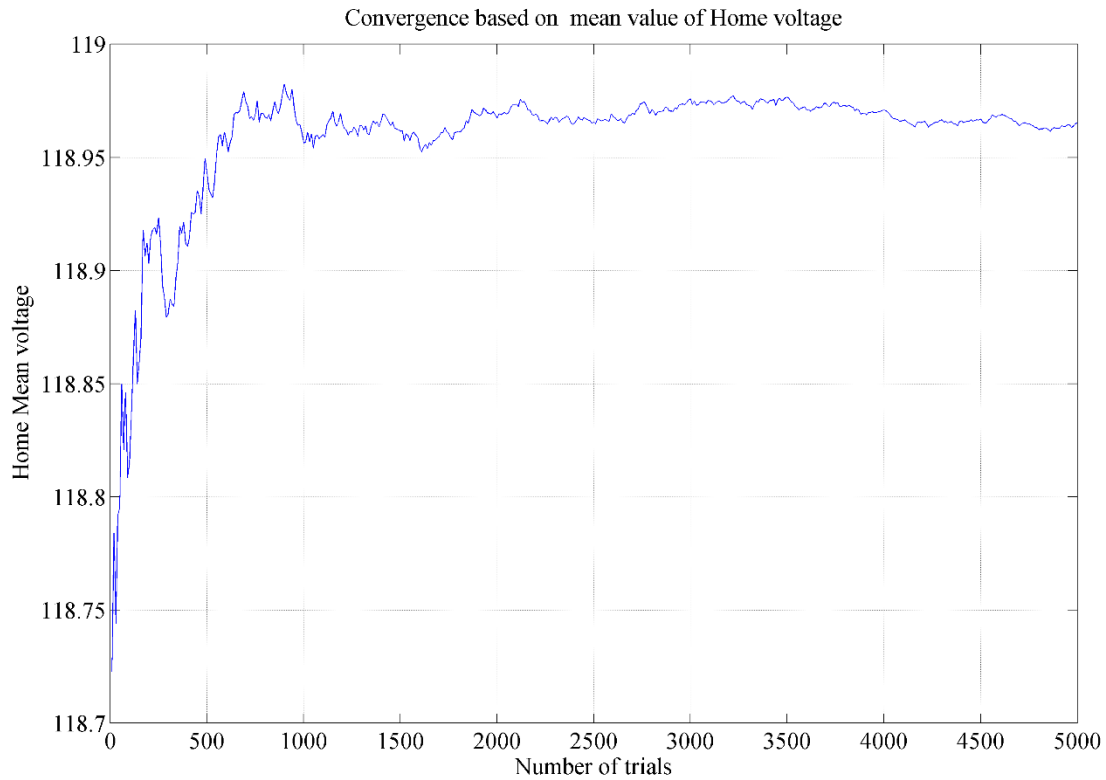


Figure 4.19: Convergence based on mean value of home voltage

Figure 4.19 illustrates the convergence based on mean value of home voltage. The value of home voltage (Scenario#6) varies from 0 to 600 trials. However, at 700 trials, the value of home voltage converges and remains almost steady until 5000 trials.

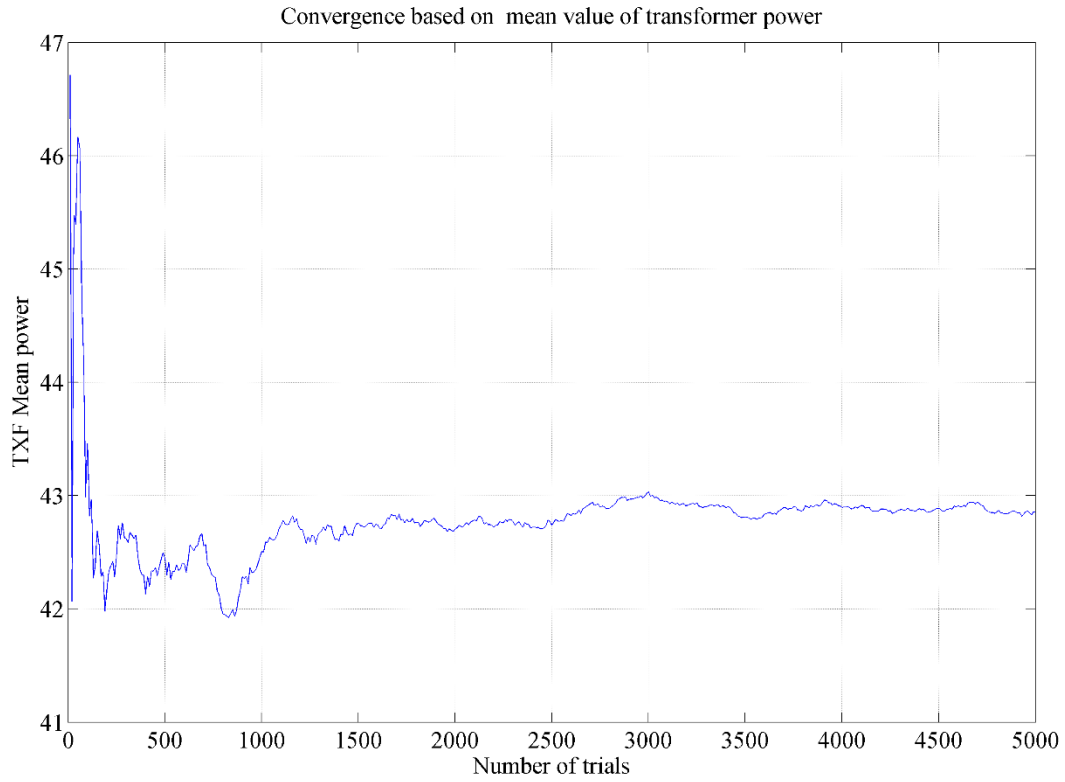


Figure 4.20: Convergence based on mean value of transformer power

The above Figure 4.20 shows the convergence based on mean value of transformer power. It is seen that the value of transformer power (Secnario#6) at 1100 trials is the convergence point, and the value remains constant towards the 5000 trials.

4.7.6.2 Loss of Life

Month	50 kVA Transformer	25 kVA Transformer	Temperature
January	2.22E-05	0.00015	-5.0167
February	1.31E-05	7.76E-05	-6.0292
March	4.32E-06	1.01E-05	-1.4208
April	0.000119	0.000135	10.1
May	0.000169	0.001585	15.175
June	0.000689	0.004835	22.458
July	0.000396	0.001881	24.292
August	0.000245	0.000597	21.7
September	0.000143	0.000319	21.488
October	3.91E-05	0.000141	11.313
November	0.000407	0.000992	4.125
December	0.000617	0.001072	-0.0125

Table 4.10: Transformer Loss of Life during the year

Table 4.10 lists the Loss of Life in 25 kVA and 50 kVA during one year. The results (in percent) shows that the monthly LOL of the 25 kVA is higher than the 50 kVA transformer. Thus, the total yearly LOL of 50 kVA and 25 kVA are 0.08737% and 0.359136% respectively.

4.8 Summary

This chapter presents six scenarios; first scenario (PV= 0 KV), second scenario (PV= 2 KV), third scenario (PV= 4 KV), fourth scenario (PV= 6 KV), fifth scenario (PV= 8 KV) and sixth scenario (PV= 10 KV) in order to investigate the effect of PVs on the house voltage and transformer power. MATLAB and Open-DSS are used to simulate the entire system. The results shows that there is no noticed influence of varying PVs on the house voltage when the transformer rate is 50 kVA. However, the house supplied from the 25KVA experience voltage variations whenever the PV rate increases. Moreover, the results did not prove that increasing the number of runs beyond 1000 trials will lead to increase the time of the processing and memory usage without any significant improvement in the obtained results as stated in [44], so some results are beyond 1000 trials. The yearly LOL of the transformer rated 50KVA decreases when the PV rate increases. However, for the transformer rated 25KVA, the yearly LOL remains almost constant even though the PV varies.

CHAPTER 5

CONCLUSION

5.1 Conclusions

Renewable energy is the energy that comes from resources which are replenish themselves and not depleted by continued use such as wind or solar power. Renewable energy has the potential to slow global warming, safe human health and reduce air pollution. Ontario's microFIT program is established to help Ontario meet its aims for improving air quality and reducing its dependence on fossil fuels.

Beside the renewable energy benefits, power quality seems to be a serious challenged. Because of the renewable energy output power intermittency in solar power generation, major power quality problems such as voltage and frequency variations are likely to occur. In order to overcome the voltage variation problem, studies presented in [28] suggested that super capacitor can be the voltage and power mitigation.

Monte Carlo simulation which is the combination of deterministic and probabilistic technique has been applied and the model of single photovoltaic cell voltage current characteristics is discussed in details. Furthermore, the convergence issue reveals that the value converges to the expected value after a large number of runs. According to [44] increasing the number of runs

beyond 1000 trials has no significant improvement in the obtained results. However, the results in this study shows some value converges beyond 1000 trials.

The IEEE 34 Bus Standard Test Distribution System has been modified by extending the secondary system and modelling the distribution transformers, secondary service lines and service drops using Open-DSS. The modification shows that 50 kVA and 25 KVA transformers configurations at nodes 822 and 846 are best to supply 10 and 6 residential houses respectively.

The secondary results have clearly shown that the house voltage experiences a variation with the 25KVA transformer whenever the PV rate increases. Inversely, the 50KVA transformer has no remarked impact of varying PVs on the house voltage.

Looking at the convergence point for both transformer power and home voltage, the results for the entire scenarios (six scenarios) reveal that the number of runs beyond 1000 trials has significant improvement in the obtained results. Lastly, the yearly LOL for the transformer rated 50KVA decreases when the PV rate increases. Nevertheless, the 25KVA transformer shows that the yearly LOL remains almost constant even though the PV varies.

References

- [1] Camacho, E. F., Samad, T., Garcia-Sanz, M., & Hiskens, I. (2011). Control for renewable energy and smart grids. *The Impact of Control Technology, Control Systems Society*, 69-88.
- [2] Mojdehi, M. N., Kazemi, A., & Barati, M. (2009, May). Network operation and reconfiguration to maximize social welfare with distributed generations. In *EUROCON 2009, EUROCON'09. IEEE* (pp. 552-557). IEEE.
- [3] Bonab, S. M. M., & Nojavan, S. Voltage Stabilization of hybrid PV and battery systems by considering temperature and irradiance changes in standalone operation.
- [4] Herzog, A. V., Lipman, T. E., & Kammen, D. M. (2001). Renewable energy sources. *Encyclopedia of Life Support Systems (EOLSS). Forerunner Volume- 'Perspectives and Overview of Life Support Systems and Sustainable Development*.
- [5] Goutard, E. (2010, October). Renewable energy resources in energy management systems. In *Innovative Smart Grid Technologies Conference Europe (ISGT Europe), 2010 IEEE PES* (pp. 1-6). IEEE.
- [6] Gonen, T. (2014). *Electric power distribution engineering*. CRC press.
- [7] Sandhu, M., & Thakur, T. (2014). Issues, Challenges, Causes, Impacts and Utilization of Renewable Energy Sources - Grid Integration.
- [8] Kumar, K. P., Venkateshwarlu, S., & Divya, G. A review on power quality in grid connected renewable energy system. *CVR JOURNAL OF SCIENCE & TECHNOLOGY*, 57.
- [9] Khadem, S. K., Basu, M., & Conlon, M. (2010). Power quality in grid connected renewable energy systems: role of custom power devices.

- [10] Baggini, A. B. (Ed.). (2008). *Handbook of power quality* (Vol. 520). Chichester: John Wiley & Sons.
- [11] Capehart, B. L., Turner, W. C., & Kennedy, W. J. (2013). *Guide to Energy Management 7th Edition*. Lulu Press, Inc.
- [12] Boyle, Godfrey ed. (2012). *Renewable Energy: Power for a Sustainable Future (3rd ed.)*. Oxford: Oxford University Press and Open University.
- [13] Stigka, E. K., Paravantis, J. A., & Mihalakakou, G. K. (2014). Social acceptance of renewable energy sources: A review of contingent valuation applications. *Renewable and Sustainable Energy Reviews*, 32, 100-106.
- [14] M. Begović, A. Pregelj, A. Rohatgi, et al., “Impact of renewable distributed generation on power systems”, in Proc. of the 34th Hawaii International Conference on System Sciences, 2001.
- [15] Ma, Y., Yang, P., & Guo, H. (2011). Distributed generation system development based on various renewable energy resources. In *Proceedings of the 30th Chinese Control Conference July* (pp. 22-24).
- [16] Zeman, M. (2003). Introduction to photovoltaic solar energy. *Delft University of Technology*, 2, 6.
- [17] Najafi, H., & Najafi, B. (2011, October). Sensitivity analysis of a hybrid photovoltaic thermal solar collector. In *Electrical Power and Energy Conference (EPEC), 2011 IEEE* (pp. 62-67). IEEE.
- [18] Thomas, R. (Ed.). (2003). *Photovoltaics and architecture*. Taylor & Francis.
- [19] More, V. P., & Kulkarni, V. V. (2014). Design and Implementation of Microcontroller Based Automatic Solar Radiation Tracker.

- [20] Knier, G. (2002). How do photovoltaics work?. *Science@ NASA*.
- [21] González-Longatt, F. M. (2005). Model of photovoltaic module in Matlab. *II CIBELEC, 2005*, 1-5.
- [22] Kalogirou, S. A. (2013). *Solar energy engineering: processes and systems*. Academic Press.
- [23] MicroFIT Program. (2015). Retrieved October 12, 2015, from http://microfit.powerauthority.on.ca/sites/default/files/microFIT_Program_Overview_version_3-2.pdf
- [24] The Ontario MicroFIT Program. (2015, April 24). Retrieved October 12, 2015, from <http://www.strandenergy.ca/the-ontario-microfit-program/>
- [25] Murali, G., & Manivannan, A. (2013). Analysis of Power Quality Problems in Solar Power Distribution System. *International Journal of Engineering Research and Applications (IJERA)*, 3(2), 799-805.
- [26] Golovanov, N., Lazaroiu, G. C., Roscia, M., & Zaninelli, D. (2013). Power quality assessment in small scale renewable energy sources supplying distribution systems. *Energies*, 6(2), 634-645.
- [27] Galzina, D. (2015). Voltage Quality Improvement Using Solar Photovoltaic System. *Journal of Sustainable Development of Energy, Water and Environment Systems*, 3(2), 140-150.
- [28] Chicco, G., Schlabbach, J., & Spertino, F. (2009). Experimental assessment of the waveform distortion in grid-connected photovoltaic installations. *Solar Energy*, 83(7), 1026-1039.
- [29] Metropolis, N., & Ulam, S. (1949). The monte carlo method. *Journal of the American statistical association*, 44(247), 335-341.

- [30] Iannone, F., Noviello, G., & Sarno, A. (1998). Monte Carlo techniques to analyse the electrical mismatch losses in large-scale photovoltaic generators. *Solar energy*, 62(2), 85-92.
- [31] Papoulis, A., & Pillai, S. U. (2002). *Probability, random variables, and stochastic processes*. Tata McGraw-Hill Education.
- [32] Rubinstein, R. Y., & Kroese, D. P. (2011). *Simulation and the Monte Carlo method* (Vol. 707). John Wiley & Sons.
- [33] Metropolis, N. (1987). The beginning of the Monte Carlo method. *Los Alamos Science*, 15(584), 125-130.
- [34] Saha, H., Bhattacharya, G., & Mukherjee, D. (1988). Mismatch losses in series combinations of silicon solar cell modules. *Solar cells*, 25(2), 143-153.
- [35] Bishop J. W. (1988) Computer simulation of the effects of electrical mismatches in photovoltaic cell interconnection. *Solar Cells* 25, 73-89.
- [36] Bucciarelli L. L. (1979) Power loss in photovoltaic arrays due to mismatch in cell characteristics. *Solar Energy* 23, 277.
- [37] Ontario Power Authority (2009). *Feed-in Tariff program* [Online]. Available: <http://microfit.powerauthority.on.ca/>
- [38] Abdelsamad, S. F., Morsi, W. G., & Sidhu, T. S. (2015). Probabilistic Impact of Transportation Electrification on the Loss-of-Life of Distribution Transformers in the Presence of Rooftop Solar Photovoltaic. *Sustainable Energy, IEEE Transactions on*, 6(4), 1565-1573.
- [39] *Environment Canada, Canadian Weather Energy Engineering Datasets (CWEEDS)* [Online]. Available: http://climate.weather.gc.ca/prods_servs/engineering_e.html
- [40] Board, I. S. (2011). IEEE guide for loading mineral-oil immersed transformers. *IEEE Std. C*, 57, 1-112.

- [41] Distribution Test Feeders. (2001). IEEE 34-Bus Standard Test Distribution System [Online]. Available: <http://ewh.ieee.org/soc/pes/dsacom/testfeeders/index.html>
- [42] Electric Power Research Institute (EPRI) (2008). *Open-DSS Simulating Environment Software* [Online]. Available: <http://sourceforge.net/projects/electricdss/files/>
- [43] Gray, M. (2013). *Probabilistic Assessment of the Impact of Plug-in Electric Vehicles on Power Quality in Electric Distribution Systems* (Doctoral dissertation, University of Ontario Institute of Technology).
- [44] Au, T. K., & Ortega-Vazquez, M. (2013, July). Assessment of plug-in electric vehicles charging on distribution networks. In *Power and Energy Society General Meeting (PES), 2013 IEEE* (pp. 1-5). IEEE.

Appendix A IEEE 34-Bus Standard Test Distribution System Data

Table A.1 Line Segment Data

Node A	Node B	Length(ft.)	Config.
800	802	2580	300
802	806	1730	300
806	808	32230	300
808	810	5804	303
808	812	37500	300
812	814	29730	300
814	850	10	301
816	818	1710	302
816	824	10210	301
818	820	48150	302
820	822	13740	302
824	826	3030	303
824	828	840	301
828	830	20440	301
830	854	520	301
832	858	4900	301
832	888	0	XFM-1
834	860	2020	301
834	842	280	301
836	840	860	301
836	862	280	301
842	844	1350	301
844	846	3640	301
846	848	530	301
850	816	310	301
852	832	10	301
854	856	23330	303
854	852	36830	301
858	864	1620	302
858	834	5830	301
860	836	2680	301
862	838	4860	304
888	890	10560	300

Table A.2 Overload Line Configurations

Config.	Phasing	Phase ACSR	Neutral ACSR	Spacing ID
300	B A C N	1/0	1/0	500
301	B A C N	#2 6/1	#2 6/1	500
302	A N	#4 6/1	#4 6/1	510
303	B N	#4 6/1	#4 6/1	510
304	B N	#2 6/1	#2 6/1	510

Table A.3 Transformer Data

	KVA	KV-high	KV-low	R - %	X - %
Substation:	25000	69 – D	24.9 – Gr. W	1	8
XFM – 1	500	24.9 – Gr. W	4.16 – Gr. W	1.9	4.08

Table A.4 Spot Loads

Node	Load	Ph-1	Ph-1	Ph-2	Ph-2	Ph-3	Ph-4
	Model	kW	kVAr	kW	kVAr	kW	kVAr
860	Y-PQ	20	16	20	16	20	16
840	Y-I	9	7	9	7	9	7
844	Y-Z	135	105	135	105	135	105
848	D-PQ	20	16	20	16	20	16
890	D-I	150	75	150	75	150	75
830	D-Z	10	5	10	5	25	10
Total		344	224	344	224	359	229

Table A.5 Regulator Data

Regulator ID:	1		
Line Segment:	814 - 850		
Location:	814		
Phases:	A – B – C		
Connection:	3-Ph, LG		
Monitoring Phase:	A – B – C		
Bandwidth:	2.0 volts		
PT Ratio:	120		
Primary CT Rating:	100		
Compensator Settings:	Ph-A	Ph-B	Ph-C
R - Setting:	2.7	2.7	2.7
X - Setting:	1.6	1.6	1.6
Voltage Level:	122	122	122
Regulator ID:	2		
Line Segment:	852 - 832		
Location:	852		
Phases:	A – B – C		
Connection:	3-Ph, LG		
Monitoring Phase:	A – B – C		
Bandwidth:	2.0 volts		
PT Ratio:	120		
Primary CT Rating:	100		
Compensator Settings:	Ph-A	Ph-B	Ph-C
R - Setting:	2.5	2.5	2.5
X - Setting:	1.5	1.5	1.5
Voltage Level:	124	124	124

Table A.6 Shunt Capacitors

Node	Ph-A	Ph-B	Ph-C
	KVAr	KVAr	KVAr
844	100	100	100
848	150	150	150
Total	250	250	250

Table A.7 Distributed Loads

Node	Node	Load	Ph-1	Ph-1	Ph-2	Ph-2	Ph-3	Ph-3
A	B	Model	kW	kVAr	kW	kVAr	kW	kVAr
802	806	Y-PQ	0	0	30	15	25	14
808	810	Y-I	0	0	16	8	0	0
818	820	Y-Z	34	17	0	0	0	0
820	822	Y-PQ	135	70	0	0	0	0
816	824	D-I	0	0	5	2	0	0
824	826	Y-I	0	0	40	20	0	0
824	828	Y-PQ	0	0	0	0	4	2
828	830	Y-PQ	7	3	0	0	0	0
854	856	Y-PQ	0	0	4	2	0	0
832	858	D-Z	7	3	2	1	6	3
858	864	Y-PQ	2	1	0	0	0	0
858	834	D-PQ	4	2	15	8	13	7
834	860	D-Z	16	8	20	10	110	55
860	836	D-PQ	30	15	10	6	42	22
836	840	D-I	18	9	22	11	0	0
862	838	Y-PQ	0	0	28	14	0	0
842	844	Y-PQ	9	5	0	0	0	0
844	846	Y-PQ	0	0	25	12	20	11
846	848	Y-PQ	0	0	23	11	0	0
Total			262	133	240	120	220	114

Appendix B Secondary System Data

Table B.1 Center Tapped Distribution Transformer Parameters

	kVA	kV-high	kV-low	R - %	X - %
Secondary 25kVA	25	4.16 - D	0.24 Gr-W	0.5367	1.0733
Secondary 50kVA	50	4.16 - D	0.24 - D	1.0140	1.7239

Appendix C Transformer Insulation Life

Aging equations:

$$\text{Per Unit Life} = A e^{\left[\frac{B}{\Theta_H + 273} \right]}$$

where

(C.1)

- Θ_H is the winding hottest-spot temperature, °C
- A is a constant
- B is a constant
- e is the base of the natural logarithm

$$F_{EQA} = \frac{\sum_{n=1}^N F_{AA,n} \Delta t_n}{\sum_{n=1}^N \Delta t_n}$$

(C.2)

where

- F_{EQA} is equivalent aging factor for the total time period
- $F_{AA,n}$ is aging acceleration factor for the temperature that exists during the time interval Δt_n
- n is index of the time interval, Δt
- N is total number of time intervals
- Δt_n is time interval, h

Percent loss of life:

$$\% \text{ Loss of life} = \frac{F_{EQA} \times t \times 100}{\text{Normal insulation life}} \quad (\text{C.3})$$

where

F_{EQA} is equivalent aging factor for the total time period